Evaluating Hr38 as a Potential Engram Marker in Drosophila

Alasdair WW Boeddinghaus

Evaluating *Hr38* as a Potential Engram Marker in *Drosophila*

Alasdair Boeddinghaus

Masters of Science by Research

Biological Sciences

2025-2026

Abstract

Long-term memory formation requires transcriptional changes within engram cells, yet labelling and manipulating engrams remains a challenge in several model species, including *Drosophila melanogaster*. In flies, olfactory memories are encoded in the Kenyon cells, which respond sparsely to odour cues. In this thesis, I explore whether expression of the activity-regulated gene *Hr38*, the fly orthologue of the mammalian *NR4A* family, reflects odour-evoked Kenyon cell activation. I first describe an automated, fluorescence-based pipeline to quantify expression of fluorescence-tagged Hr38 across 3D image stacks. Using this method, I measured a peak of Hr38 expression ~6h after odour exposure. However, this increase was not reproducible after controlling for the time of day when samples were collected. Further experiments found no increase in Hr38 expression after paired learning, unpaired learning, sugar consumption, and various odour combinations. These experiments, alongside odour-free controls, confirmed that endogenous Hr38 expression in Kenyon cells could be driven by circadian rhythms, rather than odour exposure or learning. Therefore, genetic strategies relying on *Hr38* expression are unlikely to provide a reliable way to identify odour-responsive or engram Kenyon cells.

Acknowledgements

Firstly, thank you to my supervisor, Dr Vincent Croset. I could not have asked for a better mentor and guide throughout this project. His patience, kindness and enthusiasm have been endless, and I am extremely grateful for the excitement he has helped to instil in me in this area of science.

I am grateful to Helen Siddle, whose work as lab technician made it possible for me to carry out all my experiments. Thank you to Dr Lydia Kitchen for writing the macro I used for my image analysis pipeline, and for her considerable help with my imaging. Also, to Dr Francesco Boselli, for his insights into single-cell counting methods.

A particular thank you to Gaia Pelizzatti for running the ACV experiments and the long hours that took. I am indebted to James Evans for laying the groundwork for these experiments, his deep knowledge of the science, and the informative discussions I have had with him. To Sophie, who has taught me so much this year: thank you for your encouragement, scientific input, interesting thoughts and opinions, and ultimately your friendship, which has made so much of this year a joy. Thank you to Fanila and Emily for your encouragement, practical guidance and friendship. And to the rest of the Croset Lab and Lab 20, with whom it has been a privilege to work.

Lastly to my parents, for their investment in my education and for their support throughout this degree. I would not be here without them, and I am forever grateful. And to Miles, Sebastian and Julian, who are wonderful beyond all I deserve.

Table of Contents

Introduction

The engram

One of the central aims of systems neuroscience is to identify how memories are encoded, stored, and retrieved within neural circuits. The term *engram* is now widely used to describe the physical substrate of a memory: a set of neurons and synapses that undergo experience-dependent modifications and are reactivated during recall (1). Early theoretical work proposed several core features that any engram must satisfy, including persistence over time, the capacity to be reactivated by appropriate cues, and the representation of content-specific information (2). These principles closely parallel contemporary definitions of memory traces used in experimental neuroscience.

The modern search for engram cells has been driven by the development of genetic tools that allow specific neuronal populations to be labelled, monitored, and manipulated during learning and recall (1,3). Classical conditioning paradigms, in particular, provide precise control over both the sensory cues and reinforcement signals that induce plasticity, enabling the identification of neurons whose activity is necessary for memory formation and which are sufficient to drive behavioural expression (4,5). These approaches have transformed theoretical concepts of memory storage into experimentally testable hypotheses, allowing the field to move from abstract definitions toward mechanistic understanding.

Classical conditioning

Classical conditioning is a simple but robust form of associative learning. In this paradigm, an unconditioned stimulus (US) - a stimulus that reliably evokes an automatic, innate response - is paired with a previously neutral stimulus that becomes the conditioned stimulus (CS) (6). When the CS and US are presented together, the animal begins to associate them, and after learning, the CS alone is enough to trigger the response that was originally produced only by the US (6).

Classical conditioning is widely used to study memory because it provides precise control over the timing and identity of both the sensory cue (CS) and the reinforcement signal (US) (4). This tight experimental structure produces reliable, quantifiable behavioural responses and allows investigators to define exactly when learning occurs (5). As a result, the neural pathways, synaptic plasticity mechanisms, and gene-expression changes that support memory formation can be related directly to controlled learning events. This makes classical conditioning one of the most powerful approaches for identifying and manipulating memory-encoding neurons.

Drosophila as a model to study memory and learning

The fruit fly *Drosophila melanogaster* offers a powerful genetic and neurobiological system for investigating the mechanisms of learning and memory. The *Drosophila* nervous system, though compact, contains molecular pathways and neurotransmitter systems that are highly conserved with those of vertebrates (7). This includes cyclic adenosine monophosphate (cAMP)-dependent signalling, a core intracellular signalling cascade through which neurons translate external stimuli into changes in membrane excitability and gene expression, dopamine-mediated reinforcement, during which dopamine is released to provide a positive or negative valence to the memory, and cyclic AMP response binding protein (CREB)-dependent transcriptional regulation, which promotes the expression of genes required for long-term synaptic plasticity and memory consolidation (8–13).

The fruit fly's brain is small and well-mapped, with a full connectome available which shows each neuron's location within the brain and details their connections to other neurons (14). This allows precise genetic manipulation and circuit-level analysis, enabling researchers to link specific neurons to defined behavioural outputs (15). The availability of sophisticated genetic tools, including the GAL4/UAS expression system, targeted RNA interference, optogenetics, and *in vivo* calcium imaging, permits cell-type-specific control of gene expression and neuronal activity with exceptional precision (16–19). Moreover, *Drosophila* display robust, quantifiable forms of associative learning, such as olfactory and courtship conditioning, that are comparable to mammalian paradigms of reward- and punishment-based memory

(20). Together, these advantages make *Drosophila* an informative model through which to dissect the fundamental genetic and neural mechanisms that support memory formation and persistence in a level of detail and cellular resolution that is not currently achievable in higher organisms.

In *Drosophila melanogaster*, olfactory memory is commonly tested using classical conditioning, variants of which have been designed to probe memory formation under defined temporal conditions. In a typical appetitive paradigm, starved flies are first presented with an odour alone (CS–) for two minutes, followed by a second odour (CS+) paired with sucrose (US). After 24 hours of starvation, flies choose between the two odours; a preference for the CS+ odour indicates successful learning (21). In the aversive paradigm, flies experience an odour (CS+) paired with mild electric shocks and a different odour (CS–) without shock. Repeated training sessions with rest intervals (spaced training) yield long-term aversive memory lasting more than a day (22). Because classical conditioning provides temporal precision and quantifiable behavioural readouts, it has become a key framework for identifying the neural substrates of memory in model organisms.

The *Drosophila* olfactory memory pathway

In *Drosophila*, olfactory memories are encoded in the mushroom bodies (23). The mushroom bodies are paired, bilaterally symmetrical brain structures located in the central brain. They are positioned just above the antennal lobes and are medial to the optic lobes. Composed of thousands of intrinsic neurons called Kenyon cells, whose cell bodies form a dense cluster in the dorsal posterior brain, each mushroom body extends dendrites into a cup-shaped region called the calyx, and send axons anteriorly where they bifurcate into characteristic vertical and horizontal lobes (α/β, α′/β′, and γ), giving it a distinctive stalk-and-lobes morphology that resembles a mushroom (5,24,25). During learning, odour molecules activate olfactory receptor neurons whose dendrites detect defined chemical cues (26). These neurons synapse onto olfactory projection neurons in the antennal lobe, which then transmit information to the Kenyon cells (27–29). Kenyon cells respond in an odour-specific manner, meaning that distinct odours activate different, sparse subsets of these cells

(30,31). Each Kenyon cell projects its axon into the mushroom body lobes, forming synapses with mushroom body output neurons (MBONs) that drive behavioural responses (5,32,33).

The behavioural output of the olfactory memory (either avoiding or approaching the conditioned odour) is shaped by valence, determined by dopaminergic reinforcement signals. Dopamine released from specific dopaminergic neuron (DAN) populations modifies the synaptic strength between Kenyon cells and MBONs (32–35). PPL1 DANs typically encode punishment signals, whereas PAM DANs encode reward (11,36–38). During conditioning, dopamine release at these synapses biases output pathways toward approach or avoidance, thereby linking odour representation to behavioural outcome (39).

Kenyon cells in the engram

Within the mushroom body, Kenyon cells are the principal locus of sensory integration and plasticity (11,30). The γ, α′β′, and αβ lobes contain distinct Kenyon cell subtypes defined by their input patterns and axonal projections (11,40,41). Each lobe is subdivided into compartments defined by the overlap between MBON dendrites and DAN axons. The 15 compartments participate in different stages of memory processing: broadly, the γ compartments support short-term memory, α′β′ compartments contribute to acquisition and early consolidation, and αβ compartments are required for long-term memory storage and retrieval (41–47). Among these, the γ5, α1, β1, and β2 compartments are required for the formation and expression of long-term appetitive memory (38,41,48,49).

Long-term memories (LTMs) are stabilised by the synthesis of new proteins that maintain synaptic and structural modifications including growth of new synaptic boutons, modification of postsynaptic receptor composition, structural remodelling of dendritic spines, and long-lasting changes in synaptic strength (50–53). These proteins are encoded by secondary response genes, which are activated by primary response genes - typically transcription factors rapidly and transiently induced by

neuronal stimulation (12,54–60). Such transcriptional cascades link neural activity to long-term synaptic plasticity.

The best-documented primary response gene in *Drosophila* olfactory LTM is CREB, which is upregulated in the Kenyon cells during learning and is required for LTM formation (61–64). During olfactory stimulation, projection neurons release acetylcholine onto Kenyon cells, driving calcium influx through voltage-gated calcium channels. When this calcium signal coincides with dopamine release from dopaminergic neurons, the Kenyon-cell adenylyl cyclase Rutabaga, which is activated by both calcium/calmodulin and dopamine receptor signalling, produces a rise in cAMP. Elevated cAMP activates Protein Kinase A, which in turn stimulates a mitogen-activated protein kinase (MAPK)-dependent phosphorylation of CREB. Activated CREB then induces the transcriptional programme required for the formation and stabilisation of long-term memories (65–69).

Despite significant progress in mapping the circuitry of the mushroom body and defining which Kenyon cell subtypes contribute to different forms of memory, we still lack a detailed understanding of the molecular and transcriptional processes that unfold within these neurons as they encode and store long-term memories. Synaptic plasticity in Kenyon cells is known to require new gene expression, yet the identity, timing, and regulation of the transcriptional events supporting consolidation remain only partially characterised (5,12,20,22,23,70).

Activity regulated genes and *Hr38*

Primary response genes are rapidly induced without requiring new protein synthesis and respond to a wide range of cellular stimuli. Activity-regulated genes (ARGs), by contrast, are those whose expression is driven specifically by neuronal activity. Most ARGs fall within the primary response gene category, but only a subset of primary response genes are truly activity-dependent, making ARGs a functionally defined sub-group of immediate early transcriptional responses (59,71). In mammals, ARGs such as *c-fos*, *Egr1*, and *arc* drive synaptic plasticity during memory formation and

similar genes operate in insects (72–74). In *Drosophila*, for example, *c-fos* interacts with CREB in Kenyon cells to promote long-term memory (75).

One ARG of particular interest is *Hormone receptor-like in 38 (Hr38)*, the *Drosophila* orthologue of the vertebrate *NR4A* family of orphan nuclear receptors. *Hr38* plays a crucial role in insect developmental endocrinology (76–78). It is broadly expressed during late larval, prepupal, and pupal stages, and loss-of-function mutants show fragile cuticle and defective epidermal morphogenesis, implicating *Hr38* in epidermal differentiation and metamorphosis (76–78).

In the adult nervous system, *Hr38* is thought to be rapidly induced in Kenyon cells following neuronal stimulation (70,79). Activity-linked expression of *Hr38* has been observed in the mushroom bodies of honeybees and bumblebees during foraging, a behaviour that requires continual learning and memory of floral cues, suggesting a conserved association between *Hr38* induction and experience-dependent plasticity across insects (80–82). In mammals, members of the homologous *NR4A* transcription factor family regulate plasticity-related genes such as *BDNF* and *c-Rel*, downstream of the cAMP–PKA–CREB pathway, and are themselves induced by *Mef2*, highlighting a broader evolutionary link between NR4A signalling and memory consolidation (83–86). In *Drosophila*, *Hr38* expression increases in the mushroom body after courtship conditioning and is also upregulated by *Mef2* following ethanol exposure, reinforcing the view that *Hr38* behaves as a primary response gene capable of coupling neural activation to transcriptional change (87). Despite this, the functional significance of *Hr38* induction in adult Kenyon cells remains incompletely understood. Existing *in situ* and transcriptomic studies show that *Hr38* is transiently upregulated after salient sensory or social stimuli, but they do not identify which specific stimulus types, intensities, or behavioural contexts reliably trigger this response in Kenyon cells, nor do they resolve the temporal relationship between *Hr38* mRNA and protein accumulation (70,79). However, *Hr38* is well positioned as a candidate gene whose expression may mark neurons engaged during behaviourally relevant activation in the mushroom body.

Hr38 as potential engram marker

Hr38 is a promising candidate neuronal activity marker. After stimulation via the TRPA1 ion channel, *Hr38* mRNA increases rapidly in the mushroom bodies, peaking after 90 minutes and returning to baseline within four hours (79). Its transient, activity-dependent expression makes it a potentially attractive molecular marker for identifying neurons engaged during memory formation. *Hr38* expression in Kenyon cells is induced by artificial activation of projection neurons, suggesting that odour stimulation should likewise upregulate *Hr38* specifically in the Kenyon cells responsive to that odour (79). Consequently, flies trained with a given odour may exhibit *Hr38* induction in the subset of Kenyon cells that were selectively recruited during odour processing, allowing these cells to be distinguished from non-responsive populations.

Interestingly, *Hr38* is not required for olfactory LTM (James Evans, personal communication); however, its expression could be used to identify, manipulate, and isolate engram Kenyon cells. This would allow researchers to manipulate these engram cells during behavioural tasks, and analyse the molecular signatures that distinguish them from the rest of the population while minimising interference with the memory process itself.

Project aims

I anticipate that measuring *Hr38* expression could highlight Kenyon cells that are active in response to olfactory experience, and therefore part of the engram. This study therefore aims to: (1) establish an automated image-analysis pipeline to quantify the number of Kenyon cells expressing endogenously tagged Hr38::GFP; (2) characterise the temporal patterns of endogenous *Hr38* expression in Kenyon cells following odour exposure and learning; and (3) evaluate, based on these findings, whether *Hr38* can serve as a reliable Kenyon cell engram marker.

Materials and Methods

Fly husbandry

Flies were maintained on standard cornmeal–agar medium (1% agar, 2.5% yeast, 4.73% cornmeal, 10% glucose, 1.1% Nipagin) at room temperature under a 12:12 h light–dark cycle. Crosses were kept at 18°C and 60% humidity. Flies of mixed age were used for all experiments.

Stocks and mutants

w1118;Hr38-sfGFP flies were generated by WellGenetics (New Taipei City, TW). In brief, CRISPR was used to fuse superfolder GFP (*sfGFP*) to the C-terminal end of the *Hr38* gene using a pUC57-Kan plasmid. Sequencing revealed six silent polymorphisms in the coding sequence relative to the reference genome (James Evans, personal communication). For all experiments, we used *w1118;Hr38-sfGFP;247LexA,LexAop-rcD2:RFP/MKRS* flies.

Odour exposure and brain dissections

i. 10-hour timeline protocol

Groups of ~180 mixed-sex *w1118;Hr38-sfGFP;247LexA,LexAop-rcD2:RFP/MKRS* flies were exposed in a T-maze to 1:1000 4-methylcyclohexanol (MCH) in mineral oil for 2 min. Flies were then divided into vials of ~30 individuals. One vial was placed on ice immediately for 5 min to generate the 0h timepoint group, while the remaining vials were kept at room temperature until dissection at 2, 4, 6, 8, or 10h after odour exposure (Fig. 2A).

For each timepoint, ~10 brains were dissected in ice-cold PBS + 0.5% Triton X-100. Brains were transferred into sex-separated microcentrifuge tubes containing 1mL fixative (4% paraformaldehyde in 1× PBS) and rotated for 30 min in the dark. Samples were washed twice for 1 min and three times for 10 min in PBS + 0.5%

Triton X-100, then incubated overnight at 4°C in Vectashield (VectorLabs) before mounting.

ii. Paired vs unpaired learning protocol

24 hours before the experiment, male and female *w1118;Hr38-sfGFP;247LexA,LexAop-rcD2:RFP/MKRS* flies were separated into starvation vials (25 flies/vial). On the day of dissection, groups of ~50 flies of the same sex were exposed in a T-maze to one of four conditions:

1. MCH alone (1:1000 MCH),
2. sugar alone (200% sucrose dried on Whatman filter paper),
3. paired presentation (MCH and sugar for 2 min), or
4. unpaired presentation (sugar for 2 min, 45 s rest, MCH for 2 min) (Fig. 3B).

Flies were then divided into two groups: one placed on ice immediately (0h timepoint group), and one left at room temperature for 6h before dissection (6h timepoint group) (Fig. 3A).

Brains were dissected as in the 10h timeline protocol. All conditions were dissected on the same day, with exposure order rotated across days to control for circadian effects (Fig. 3C).

iii. Double odour exposure protocol

42-66 hours before the experiment, male and female *w1118;Hr38-sfGFP;247LexA,LexAop-rcD2:RFP/MKRS* flies were separated into fresh food vials (25 flies/vial). On the day of dissection, groups of ~50 flies of the same sex were exposed in a T-maze to one of three conditions:

1. MCH alone (1:1000),
2. Isoamyl acetate (IAA) alone (1:1000), or
3. MCH and IAA together (1:1000 each).

Flies were then divided into two groups: one placed on ice immediately (0h timepoint group) and one left at room temperature for 6h before dissection (6h timepoint group) (Fig. 4A).

Brains were dissected as in the 10h timeline protocol. All conditions were dissected on the same day, with exposure order rotated across days to control for circadian effects (Fig. 4B).

iv. Complex odour exposure protocol

42-66 hours before the experiment, male and female *w1118;Hr38-sfGFP;247LexA,LexAop-rcD2:RFP/MKRS* flies were separated into fresh food vials (25 flies/vial). On the day of dissection, groups of ~50 flies of the same sex were exposed in a T-maze to one of two conditions:

1. MCH alone (1:1000), or
2. undiluted apple cider vinegar (ACV).

Flies were divided into two groups: one placed on ice immediately (0h timepoint group) and one left at room temperature for 6h before dissection (6h timepoint group) (Fig. 5A).

Brains were dissected as in the 10h timeline protocol. Both conditions were dissected on the same day, with exposure order rotated across days to control for circadian effects (Fig. 5B).

v. No odour at different times of day protocol

42-66 hours before the experiment, male and female *w1118;Hr38-sfGFP;247LexA,LexAop-rcD2:RFP/MKRS* flies were separated into fresh food vials (25 flies/vial). On the day of dissection, groups of ~50 flies of the same sex were placed in a T-maze under odour-exposure conditions, but with no odour delivered. Groups were exposed at 8:00h, 10:00h, or 12:00h.

For each timepoint, flies were divided into two groups: one placed on ice immediately (0h timepoint group) and one left at room temperature for 6h before dissection (6h timepoint group) (Fig. 6A).

Brains were dissected as in the 10h timeline protocol.

Microscopy

Brains were mounted in Vectashield (VectorLabs) between two strips of electrical tape on a glass slide and covered with a glass coverslip. Brains were aligned dorsal side up and ventral side down, with the posterior face upwards.

Kenyon cells were imaged on a Zeiss LSM 800 confocal microscope using a 63× objective. Damaged or misoriented brains were excluded. The red channel (RFP-labelled Kenyon cell membranes) was used to define imaging regions, and Z-stacks encompassed all Kenyon cells in the mushroom body calyx. To ensure consistency, only the right calyx was analysed, although no qualitative differences were observed between hemispheres. Male and female brains were imaged separately, but data were pooled since no sex differences in *Hr38* expression were detected.

i. Original microscope settings

For the 10h timeline experiments, TuRFP (553/573 nm) and EGFP (488/509 nm) lasers were used to image Kenyon cell membranes (red) and *Hr38* expression (green), respectively. Images were acquired at 0.33 × 0.33 × 0.9 µm resolution with 16-bit depth, scan speed 6 (bidirectional), and frame-by-frame scanning. Detector gain was 905 V for both lasers, with digital gain set to 1.0 (TuRFP) and 4.0 (EGFP). Pinhole size was 5 AU for both tracks. Airyscan processing was applied post-acquisition. These settings produced sufficient resolution but required long acquisition times.

ii. Optimised microscope settings

Subsequent experiments used optimised settings for faster acquisition while maintaining resolution. TuRFP (553/573 nm) and suGFP (488/509 nm) lasers were used to image Kenyon cell membranes (red) and *Hr38* expression (green), respectively. Images were acquired at 0.085 × 0.085 × 0.9 µm resolution with 16-bit depth, scan speed 7 (bidirectional), and frame-by-frame scanning. Detector gain was set to 905 V (suGFP) and 822 V (TuRFP), with digital gain 1.0 for both. Pinhole size was 1 AU (suGFP) and 0.89 AU (TuRFP). Airyscan processing was not applied.

TrackMate parameters

i. Measuring average fluorescence in activated and not-activated cells

To quantify fluorescence, three images from independent experiments were analysed from flies exposed to MCH for 2 min and dissected 6h later, when GFP signal was highest (Fig. 2B). Images were pre-processed with background subtraction and Gaussian blur. In the green channel, cells visually identified as *active* (higher Hr38::GFP than surrounding cells) were randomly selected, and regions of interest (ROIs) were drawn around them (Fig. 1B). Average fluorescence (RFU) was measured for 20 active cells per image across Z-stacks.

Not-active cells were identified using the red membrane channel to locate Kenyon cells. ROIs were placed over candidate cells, then switched to the green channel to verify fluorescence (Fig. 1B). Cells with clear activation were excluded; otherwise, mean RFU was recorded. Twenty not-active cells were measured per image.

The procedure was repeated with the same images after acquisition under optimised microscope settings, using identical analysis parameters.

ii. Preparing images for running the Kenyon cell ROI macro

For ROI generation, the red channel contrast and brightness were manually adjusted in FIJI to over-saturate the calyx and reveal all Kenyon cell regions. Maximum contrast was set to ~600 pixel values (original settings) or ~3000 pixel values (optimised settings).

iii. Using TrackMate to count Hr38::GFP+ cells

The TrackMate plugin was used to count cells in the green channel once regions outside the mushroom body had been excluded. Firstly, background subtraction was applied with a rolling ball radius of 50 pixels, with all other optional settings left

unapplied. A Gaussian blur filter was then applied. The DoG detector was selected, with the estimated object diameter set to 4.5 μm and the initial quality threshold set to the automatically applied setting of 22.552. This threshold was applied to reduce the number of detected spots and prevent Fiji from exceeding memory limits. Median filtering was disabled and sub-pixel localisation was enabled.

After running the preview to detect initial spots, filters were applied to restrict detections to cells containing above-basal levels of Hr38::GFP. The Mean Intensity filter was set, and the Quality filter was further refined to retain only spots corresponding to Hr38::GFP+ cells (see Results, Chapter 1, Section iii).

Memory protocols

i. Heat-shock testing of wild-type flies

Memory experiments were performed in a vertical T-maze at 20–25 °C under variable humidity. Appetitive LTM was assayed following Krashes and Waddell with minor modifications (88). Flies were starved for 22–24 h in 1% agar vials before training.

During training, ~100 flies were loaded into the CS– tube (Whatman paper moistened and dried). Flies were exposed for 2 min to either 1:1000 4-methylcyclohexanol (MCH) or 1:1000 isoamyl acetate (IAA), followed by 30s of clean air. They were then transferred into the CS+ tube (Whatman paper coated with dried 200% sucrose solution) and exposed for 2 min to the alternative odour. Flies were removed from the T-maze and starved again for 22–24h.

Approximately 20h after training, flies were split into four groups. Three groups were heat-shocked at 37 °C for 1h, while one group remained untreated. The first group was tested for memory directly after the hour of heat-shock had elapsed (0h group), the second group was tested an hour later (1h group), the third group was tested an hour after that (2h group), and the final group was tested in the gaps between the other groups spread over three hours (No HS group).

For testing, flies were loaded into the T-maze elevator in darkness and allowed to choose for 2 min between tubes containing MCH or IAA odour streams. The number of flies in each tube was counted.

Performance index (PI) was calculated as:

$$PI = \frac{CS^- - CS^+}{CS^- + CS^+}$$

Statistics

For dissection experiments, differences in Hr38::GFP+ Kenyon cell numbers were tested using Kruskal-Wallis tests with Bonferroni-adjusted pairwise comparisons. For memory experiments, PI scores were analysed using one-way ANOVA with Dunnett's post hoc tests. Statistical significance was defined as $p \leq 0.05$. All analyses were performed in R.

Results

To determine whether *Hr38* can be used as a marker of odour-responsive Kenyon cells, I examined whether its expression reflected the expected pattern of activity in these neurons. Because distinct, sparse populations of Kenyon cells respond to individual odours, a corresponding subpopulation would be expected to show increased *Hr38* expression following odour presentation (89). If *Hr38* functions as an activity marker in the mushroom body, its expression should therefore be restricted to approximately 100-200 Kenyon cells, consistent with their sparse activation by odours (30,90).

Chapter 1: A method to count Hr38::GFP-positive Kenyon cells

i. Manual quantification of Hr38::GFP+ Kenyon cells

To quantify changes in the number of Hr38::GFP+ Kenyon cells following odour exposure, I established a method to visualise and quantify Hr38 within these cells. The Croset lab generated a fly line expressing Hr38 fused to GFP at the C-terminus, and crossed these flies to 247-LexA, LexAop-rcd2:RFP to label Kenyon cell membranes (91). The resulting flies enabled simultaneous visualization of endogenous Hr38 and Kenyon cell membranes (Fig. 1A).

Even during sleep, many neurons exhibit spontaneous firing and homeostatic gene expression (92,93). This is especially likely to be true in neurons involved in the memory circuitry, which need to be primed for plasticity (94,95). Consequently, Hr38 is expressed at basal levels in whole brains and individual brain regions (79,96,97). I therefore developed an image analysis pipeline to distinguish basal Hr38 expression from activity-dependent Hr38 increases induced by odour exposure in Kenyon cells.

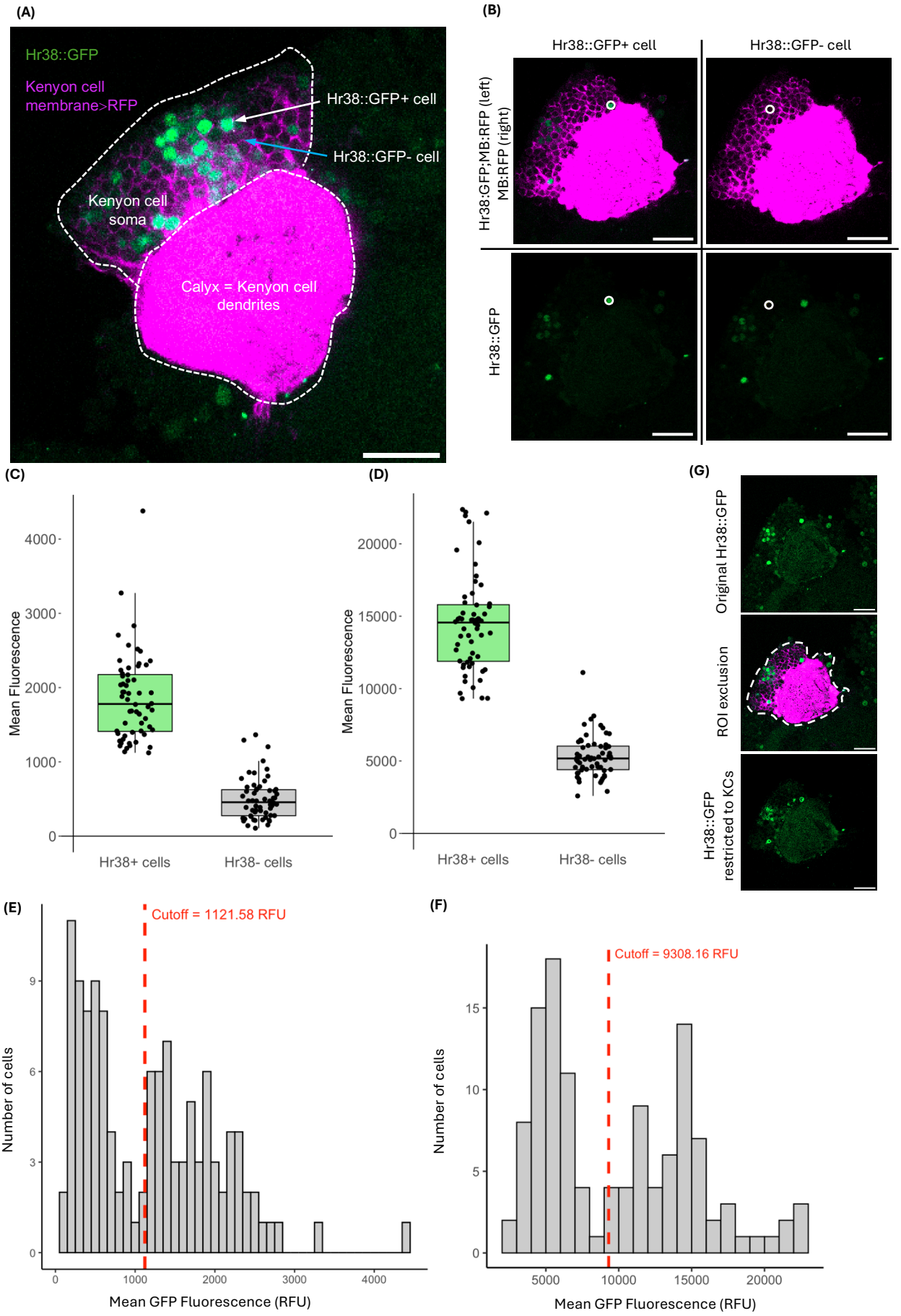

Figure 1: Establishing a fluorescence-based pipeline to identify Hr38::GFP-positive Kenyon cells. (A) Example image representing Hr38::GFP expression in

Kenyon cells. **(B)** Example of Hr38::GFP+ and Hr38::GFP- Kenyon cells. The circles represent where a ROI was drawn when measuring average cell fluorescence. **(C-D)** Average cell fluorescence levels between cells deemed Hr38::GFP+ and Hr38::GFP- using images taken before (C) and after (D) microscope settings optimisation (n=60 cells across 3 images). **(E-F)** Histograms of the mean fluorescence levels in cells used to determine a suitable cutoff point for Hr38::GFP+ vs Hr38::GFP- cells before (E) and after (F) microscope optimisation settings. The red line indicates the fluorescence level above which cells were considered Hr38::GFP+ (n=60 cells across 3 images)**. (G)** The ROI macro excludes all areas from the Hr38::GFP channel which do not overlap with the MB::RFP channel. **(A, B, G)** The green channel shows *Hr38::sfGFP* and the magenta channel shows *MB247-LexA, LexAop-rCD2::RFP.* Scale bars = 20μm.

As a first step in developing an automated image analysis pipeline for quantifying Hr38::GFP+ Kenyon cells, I manually annotated fluorescence levels to establish criteria that would distinguish Hr38::GFP+ from Hr38::GFP- Kenyon cells. I measured average GFP fluorescence in Kenyon cells 6h after flies were exposed to 1:1000 MCH for 2 min. I looked at the green channel of images and decided whether or not the GFP was bright enough to make the cell visible. Cells which were visible were classified as Hr38::GFP+ and those which were not were classified as Hr38::GFP- (Fig. 1A,B). The minimum value among Hr38::GFP+ cells (1121.58 RFU) was set as the cutoff for GFP-positive classification, as most Hr38::GFP- cells fell below this threshold (Fig. 1C,E). This cutoff was applied in TrackMate analyses to exclude cells with fluorescence below 1121.58 RFU (see section iii) (98). This quantification process was repeated when the image acquisition settings were optimised on the microscope (see Methods). This time the minimum value for Hr38::GFP+ cells of 9308.16 RFU was used as the cutoff for Hr38::GFP+ cells (Fig.1D,F).

ii. Defining a region of interest

To restrict analysis to Kenyon cells, Hr38::GFP signal outside the mushroom body was excluded. The red channel was adjusted to oversaturate the calyx, ensuring all Kenyon cell regions were visible. An ImageJ macro (kindly provided by Dr Lydia Kitchen) was used to exclude non-saturated regions, leaving only the Kenyon cell soma and calyx as a region of interest. This ROI was overlaid onto the GFP channel for each Z-stack slice, resulting in GFP signal restricted to Kenyon cells (Fig. 1E).

iii. TrackMate optimisation for counting Hr38::GFP+ cells

Hr38::GFP+ cells were quantified using FIJI's TrackMate plugin (98). The Difference of Gaussians (DoG) detector, which is optimised for detecting small, bright objects against a dark background, was applied for initial spot identification. The Mean Intensity filter was set to exclude spots below the intensity cutoffs established above (Fig. 1C,D). Then, a quality threshold was applied to further eliminate non-cellular detections. To calibrate detection thresholds, TrackMate thresholds were then adjusted until automated counts were as similar as possible to manual counts.

Chapter 2: Using *Hr38* as an engram marker

i. Temporal dynamics of odour-induced Hr38 expression in Kenyon cells

My first objective was to quantify Hr38 levels in Kenyon cells over time following exposure to an odour. I exposed *Hr38-sfGFP;247LexA,LexAop-rcD2:RFP* flies to 1:1000 MCH for 2min in a vertical T-maze setup, and dissected brains immediately, and at 2h intervals up to 10h (Fig. 2A).

As *Hr38* is rapidly and transiently expressed in response to neuronal activity, I expected Hr38::GFP+ cell numbers to peak around 2h after odour exposure, and return to baseline by 6h (70,79,99). Interestingly, the peak occurred more slowly than anticipated, with the maximum number of Hr38::GFP+ Kenyon cells observed 6h following odour exposure. By 10h, Hr38::GFP+ cell numbers had returned to basal levels, showing no significant difference compared to 0h (Fig. 2B,C). This decline took ~4h, which is what I expected.

Although my results suggest that odour exposure triggered Hr38 expression in a subset of Kenyon cells, the raise in Hr38::GFP levels occurred more slowly than anticipated. This delay may reflect reduced turnover of the larger fusion protein, but could also result from sustained Hr38 expression following prolonged or secondary cellular processes triggered by odour exposure. The number of Hr38::GFP+ cells

was also higher than anticipated. Each mushroom body hemisphere contains ~2,000 Kenyon cells, and odour responses are typically sparse, with only ~5–10% of Kenyon cells activated by a given odour (90). Thus, the observed peak of ~207 Hr38::GFP+ cells at 6h was at the upper boundary of this expected range.

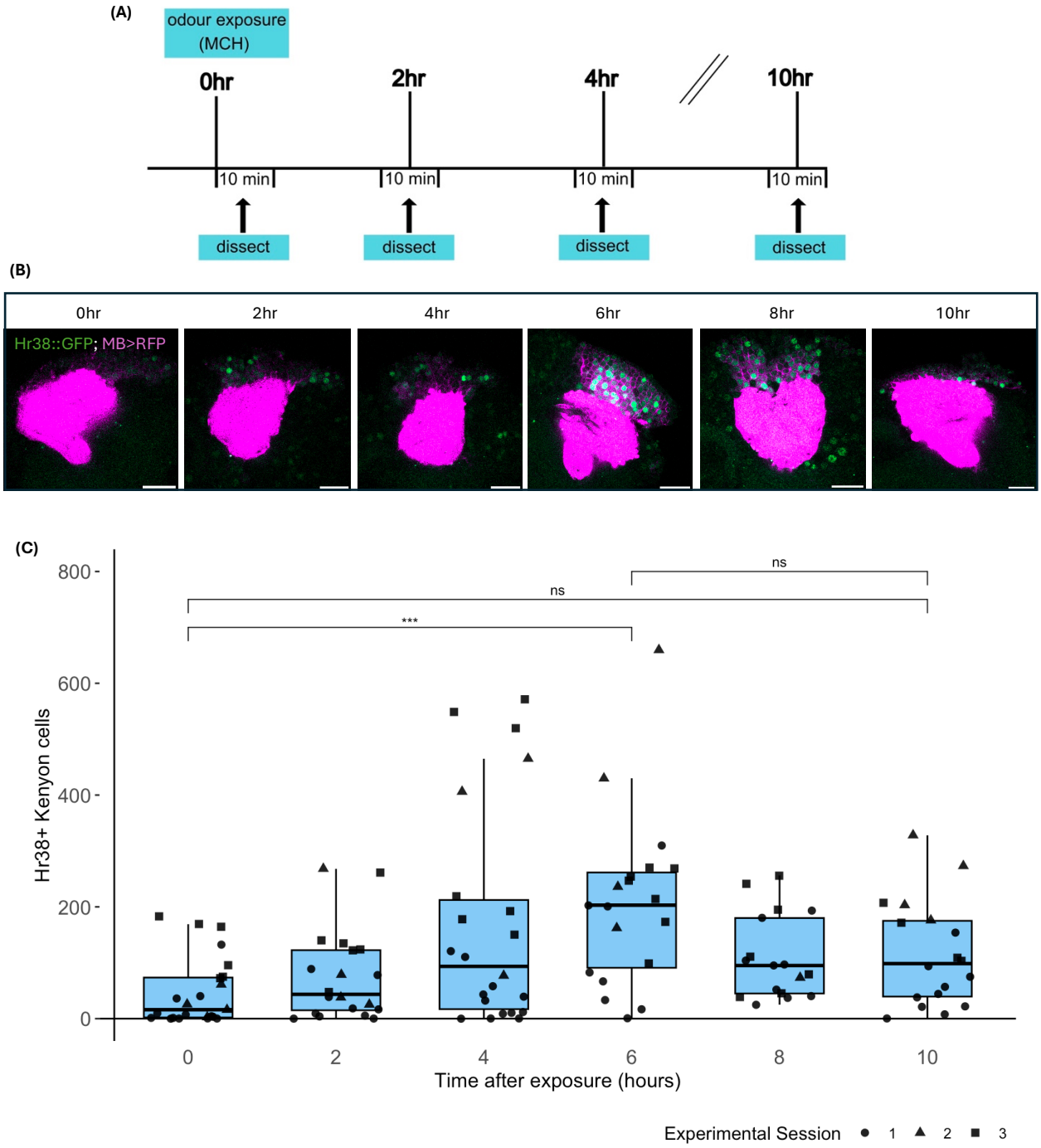

Figure 2: Hr38::GFP expression in Kenyon cells peaks 6 hours after odour exposure. (A) Experimental design. Flies were exposed to 1:1000 MCH for 2 min in a T-maze, and brains were dissected immediately and at 2h intervals up to 10h. **(B)** Representative images of brains dissected at each time point. Green, Hr38::sfGFP.

Magenta, MB247-LexA, LexAop-rCD2::RFP. Scale bar, 20μm. **(C)** Number of Hr38::GFP+ Kenyon cells at each time point. ***: $p < 0.001$ (Kruskal–Wallis test); n = 23, 20, 22, 19, 17, 18 calyxes for 0, 2, 4, 6, 8, and 10h, respectively (across three experimental sessions). Box plots show minimum, Q1, median, Q3, and maximum values. Each point represents Hr38::GFP+ cell number from the right-hand calyx of one brain. Different point shapes indicate independent experimental sessions.

ii. Hr38 expression in Kenyon cells in the context of learning

I next examined whether Hr38 induction in Kenyon cells differs during paired or unpaired learning compared to odour exposure alone. In paired learning, dopamine is released at Kenyon cell/MBON synapses concurrently with odour-evoked Kenyon cell activity (90). This coincident release modifies synaptic strength and underlies associative learning (100). In contrast, during unpaired learning, dopamine release occurs before or after odour-evoked Kenyon cell activity, and synaptic modulation does not take place (101).

I did not expect dopamine release to directly influence Hr38 dynamics. *Hr38* is upregulated in response to neuronal activity, and dopamine acts postsynaptically at the Kenyon cell/MBON synapse rather than generating activity in Kenyon cells themselves (35,70,100,102). Nonetheless, it was important to investigate whether there are any differences in Hr38::GFP expression between paired and unpaired learning, as this would affect its reliability as an engram marker.

I compared Hr38::GFP+ cell numbers across four conditions: (i) exposure to MCH alone; (ii) exposure to sugar alone; (iii) paired conditioning; and (iv) unpaired conditioning (Fig. 3A,B). The number of Hr38::GFP+ Kenyon cells did not differ among the paired conditioning group and the unpaired conditioning group at 6h (Fig. 3D,E). In fact, in this experiment, no significant change was observed between 0h and 6h in any condition (Fig. 3D,E). These results contrast with my previous experiments (Fig. 2B), where Hr38::GFP+ Kenyon cell numbers increased 6h after MCH exposure. The fact that even the odour-only control did not recapitulate the previously observed increase in Hr38 levels suggests that an uncontrolled variable might influence Hr38 expression.

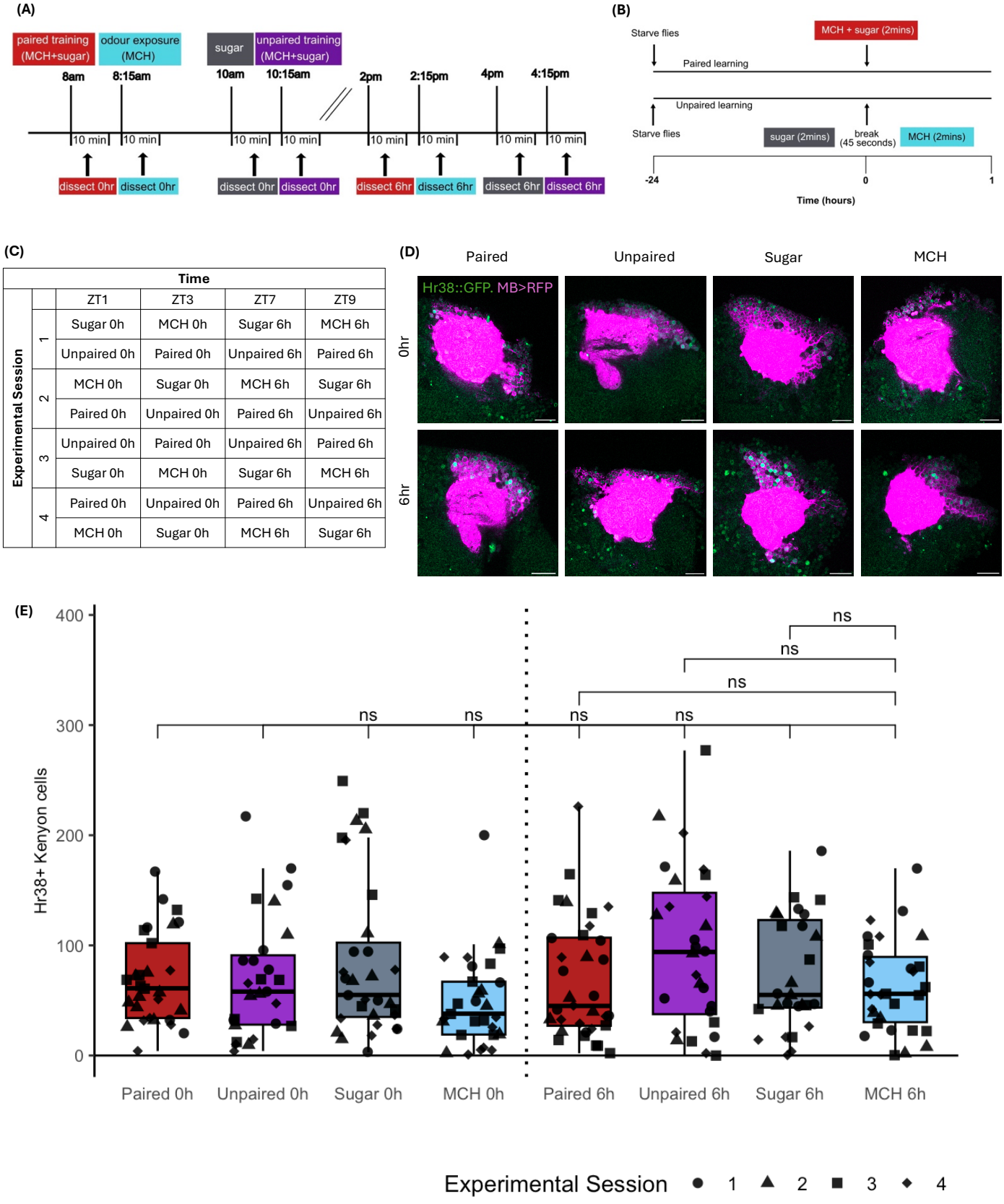

Figure 3: Hr38::GFP expression does not differ between paired and unpaired learning conditions. (**A**) Experimental design. (**B**) Paired and unpaired conditioning protocols. All flies were starved for 24h prior to exposure. (**C**) Timings for dissections. At the 0h timepoints (ZT1 and ZT3) flies were exposed to the condition and brains

were dissected straight away. At the 6h timepoints (ZT7 and ZT9) flies were dissected. Experiments on paired and unpaired groups were conducted at slightly staggered intervals (on the hour vs ~15 min later). (**D**) Representative images of brains dissected at 0h and 6h for each condition. Green, Hr38::sfGFP. Magenta, MB247-LexA, LexAop-rCD2::RFP. Scale bar, 20µm. (**E**) Number of Hr38::GFP+ Kenyon cells across paired, unpaired, sugar-only, and MCH-only groups. ns: $p > 0.05$ (Kruskal–Wallis test; Bonferroni correction). Sample sizes: paired 0h, n = 29; paired 6h, n = 33; unpaired 0h, n = 26; unpaired 6h, n = 28; sugar 0h, n = 30; sugar 6h, n = 26; MCH 0h, n = 28; MCH 6h, n = 29 (across four experimental sessions). Boxplots show minimum, Q1, median, Q3, and maximum values. Each point represents Hr38::GFP+ cell number from the right-hand calyx of one brain. Different shapes indicate independent experimental sessions.

iii. Hr38::GFP+ Kenyon cell numbers following simultaneous exposure to two odours

To further test whether the increased Hr38::GFP levels in the timeline experiment (Fig. 2B) reflects odour-evoked activity in Kenyon cells, I exposed flies to a mix of two odours (Fig. 4A). I reasoned that if Hr38 expression marks odour-responsive Kenyon cells, the mixture would be expected to trigger neuronal responses in a larger fraction of cells and yield a greater number of Hr38::GFP+ cells than either odour alone (30,31,103).

I exposed flies to a blend of 1:1000 MCH and 1:1000 IAA and dissected their brains 6h later. In these flies, Hr38::GFP+ Kenyon cell counts were similar to those in flies exposed to either odour alone (Fig. 4C,D). This suggests that Hr38 levels do not reflect the additive activation of two distinct odour-responsive populations and may not be reporting odour-driven activity.

(A)

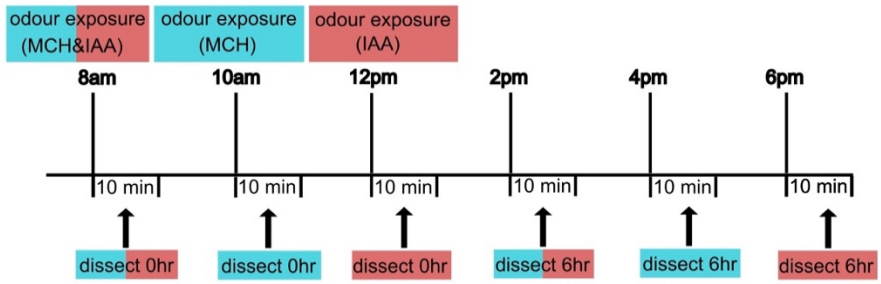

(B)

		Time					
		ZT1	ZT3	ZT5	ZT7	ZT9	ZT11
Experimental Session	1	MCH & IAA 0h	IAA 0h	MCH 0h	MCH & IAA 6h	IAA 6h	MCH 6h
	2	IAA 0h	MCH 0h	MCH & IAA 0h	IAA 6h	MCH 6h	MCH & IAA 6h
	3	MCH & IAA 0h	MCH 0h	IAA 0h	MCH & IAA 6h	MCH 6h	IAA 6h
	4	MCH 0h	MCH & IAA 0h	IAA 0h	MCH 6h	MCH & IAA 6h	IAA 6h
	5	MCH & IAA 0h	IAA 0h	MCH 0h	MCH & IAA 6h	IAA 6h	MCH 6h
	6	IAA 0h	MCH 0h	MCH & IAA 0h	IAA 6h	MCH 6h	MCH & IAA 6h

(C)

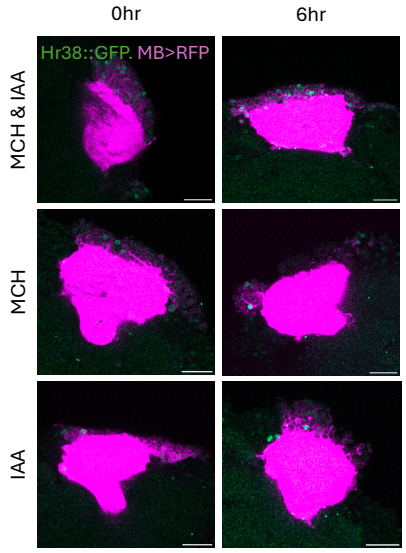

(D)

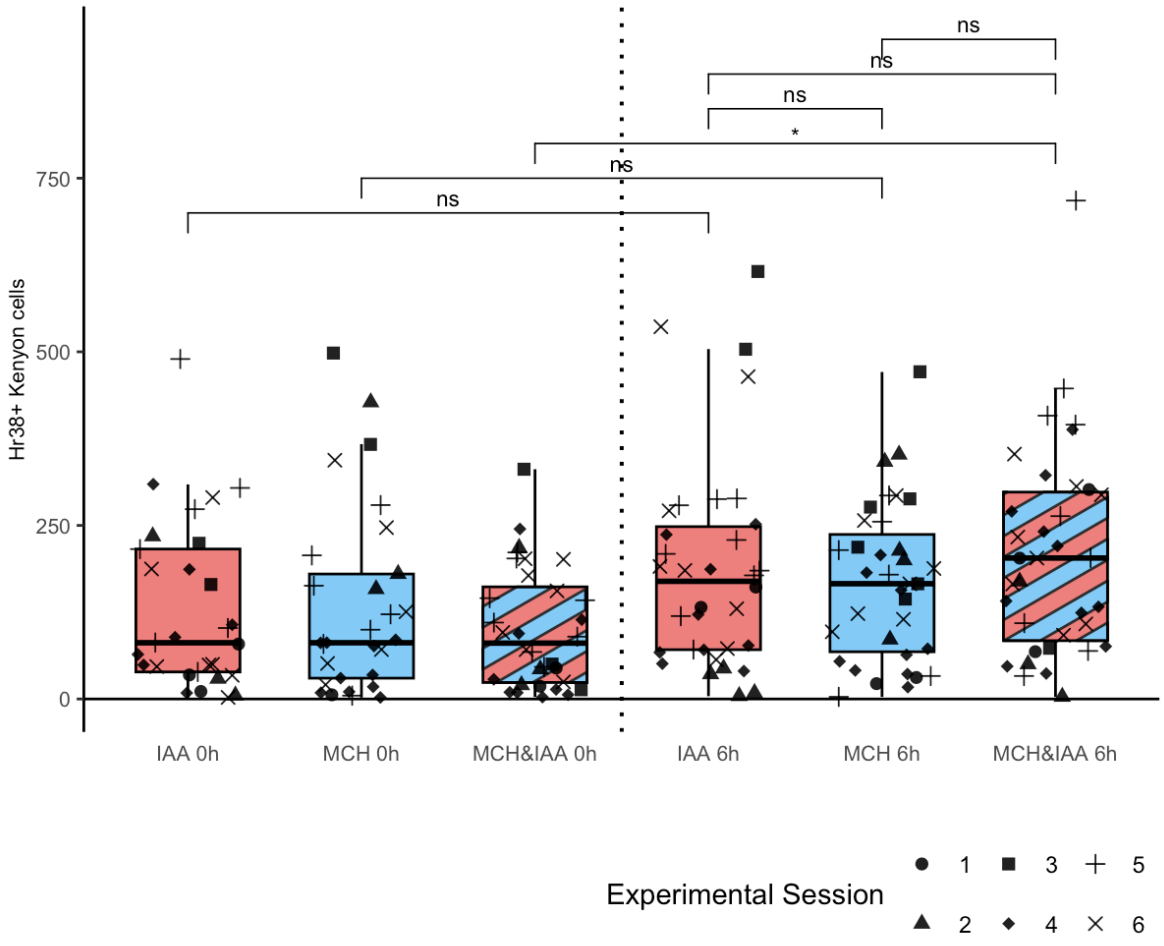

Figure 4: Simultaneous exposure to two odours does not increase Hr38::GFP-positive Kenyon cell numbers. (**A**) Experimental design. (**B**) Timing of experimental sessions. At the 0h timepoints (ZT1, ZT3 and ZT5) flies were exposed to the condition and brains were dissected straight away. At the 6h timepoints (ZT7, ZT9 and ZT11) flies were dissected. (**C**) Representative images of brains dissected at 0h and 6h for each condition. Green, Hr38::sfGFP. Magenta, MB247-LexA, LexAop-rCD2::RFP. Scale bar, 20µm. (**D**) The number of Hr38::GFP+ Kenyon cells between flies exposed to both MCH and IAA, or to either odour alone. No significant difference was detected at 6h between the mixture and single-odour groups. ns: $p > 0.05$ (Kruskal–Wallis test; Bonferroni correction). Sample sizes (across six experimental sessions): IAA 0h, n = 28; MCH 0h, n = 28; MCH+IAA 0h, n = 34; IAA 6h, n = 34; MCH 6h, n = 33; MCH+IAA 6h, n = 34 (across six experimental sessions). Boxplots show minimum, Q1, median, Q3, and maximum values. Each point represents Hr38+ cell number from the right-hand calyx of one brain. Different shapes indicate independent experimental sessions.

Interestingly, flies exposed to the odour mixture showed a significant increase in Hr38::GFP+ cells between 0h and 6h, whereas no such change was observed with either odour alone (Fig. 4C,D). This could indicate that exposure to a more complex odour stimulus results in the recruitment of a greater number of Kenyon cells. However, this experiment still did not match the results from the timeline experiment where Hr38::GFP+ cells increased from 0h to 6h following exposure to MCH (Fig. 2B,C). Therefore, there might be an uncontrolled variable which is causing the difference in the number of Hr38::GFP+ cells between the 0h and 6h timepoints in the MCH+IAA group.

iv. Hr38 expression in Kenyon cells following exposure to a complex odour

To test whether the higher number of Hr38::GFP+ cells observed after simultaneous exposure to two odours (Fig. 4D) reflected recruitment of additional Kenyon cells by a more complex stimulus, I exposed flies to a natural chemical mixture. Unlike MCH or IAA which are pure chemical compounds, apple cider vinegar (ACV), contains multiple odorants, including acetic acid, ethyl acetate, acetaldehyde, and methanol (104). A mixture such as ACV is expected to activate a broader range of olfactory receptor neurons and thereby recruit a larger population of Kenyon cells (105,106).

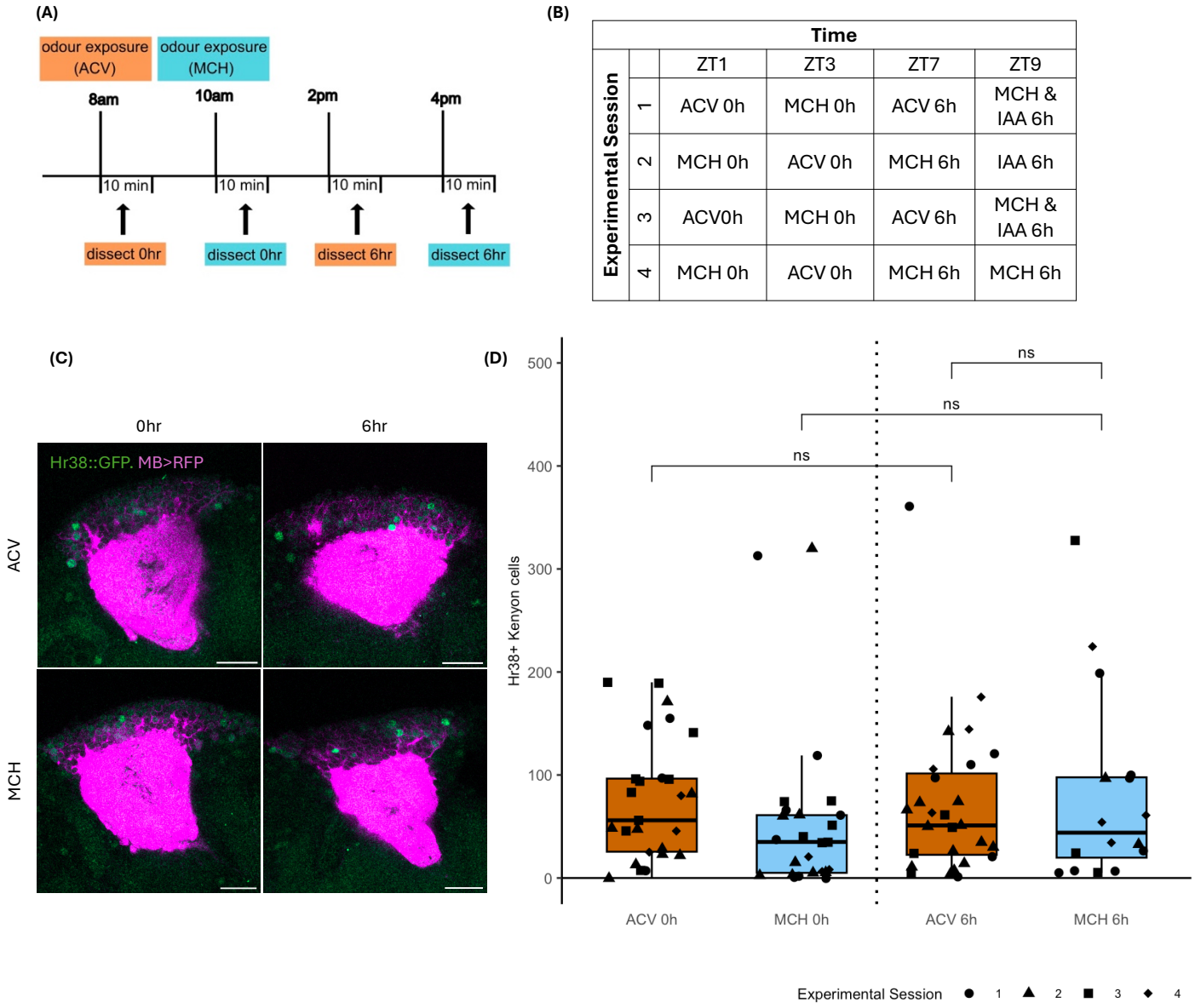

Figure 5: Complex odour exposure does not increase Hr38::GFP-positive Kenyon cell recruitment. (**A**) Experimental design. (**B**) Timing of experimental sessions. At the 0h timepoints (ZT1 and ZT3) flies were exposed to the condition and brains were dissected straight away. At the 6h timepoints (ZT7 and ZT9) flies were dissected. (**C**) Representative images of brains dissected at 0h and 6h for each condition. Green, Hr38::sfGFP. Magenta, MB247-LexA, LexAop-rCD2::RFP. Scale bar, 20µm. (**D**) The number of Hr38::GFP+ Kenyon cells between ACV- and MCH-exposed flies. ns: $p > 0.05$ (Kruskal–Wallis test; Bonferroni correction). Sample sizes: ACV 0h, n = 26; MCH 0h, n = 24; ACV 6h, n = 26; MCH 6h, n = 15 (across four experimental sessions). Boxplots show minimum, Q1, median, Q3, and maximum values. Each point represents Hr38::GFP+ cell number from the right-hand calyx of one brain. Different shapes indicate independent experimental sessions.

These experiments were conducted by Gaia Pelizzatti, a summer intern in the Croset lab. Unlike the MCH and IAA blend, ACV exposure did not elicit an increase of Hr38::GFP+ Kenyon cell numbers, and these flies had comparable Hr38::GFP+ Kenyon cell counts as those exposed to MCH (Fig. 5C,D). Once again, we did not measure any difference in Hr38::GFP+ Kenyon cell numbers between the 0h and 6h timepoints in MCH exposed flies (Fig. 5C,D).

Prior calcium studies strongly suggest that Kenyon cell recruitment is broader and more cells are activated in response to complex odours than to simple synthetic odours (31,89,107). In contrast, our data indicate that the number of Hr38::GFP+ Kenyon cells does not increase following exposure to ACV or to a mixture of MCH and IAA, relative to MCH alone (Figs. 2C, 4D, 5D). This discrepancy suggests that Hr38::GFP may not reliably report odour-evoked activity in Kenyon cells.
However, the timeline experiment revealed a clear increase in Hr38::GFP+ cells between 0h and 6h (Fig. 2C), an effect not reproduced in any other experiment comparing these time points after MCH exposure (Figs. 3E, 4D, 5D). One key uncontrolled variable in the timeline experiment was the time of day at which flies were exposed to odour. All flies were trained at approximately ZT1, meaning that the 0h time point corresponded to ZT1 and the 6h time point to ZT7. In later experiments, exposure times were rotated across independent sessions to avoid confounding effects of circadian phase (Figs. 3C, 4B, 5B). I therefore hypothesised that the increase in Hr38::GFP+ cells between 0h and 6h observed in the timeline experiment reflects circadian modulation of Hr38 expression, rather than the upregulation of Hr38 in response to odour-evoked activity in the Kenyon cells. This interpretation also accounts for the increase seen between 0h and 6h in flies exposed to the MCH+IAA mixture (Fig. 4D), since this group was exposed at ZT1 in three separate replicates, whereas the MCH-alone and IAA-alone groups were trained at ZT1 only once or twice, respectively (Fig. 4B).

v. Hr38 expression in Kenyon cells is circadian

To test whether Hr38 induction depends on the time of the day, I exposed flies to room air without odour at different time points. Flies were introduced to the T-maze at ZT1, ZT3 or ZT5 (08:00, 10:00 or 12:00h) and dissected immediately or 6h later (Fig.

6A). These timepoints corresponded to the times at which flies were exposed to odours in the other experiments (Figs. 2A, 3A, 4A, 5A).

The number of Hr38::GFP+ Kenyon cells increased significantly from 0h to 6h in the group of flies which were introduced to the T-maze at ZT1, but not those introduced at ZT3 or ZT5 (Fig. 6B,C). These results indicate that the number of Hr38::GFP+ Kenyon cells depends on circadian timing, rather than odour exposure.

This result provides a likely explanation for the increase observed between 0h and 6h in the timeline experiment, which did not control for time of day (Fig. 2A,B). In that experiment, all flies were exposed to odour around ZT1 (between 07:55h and 08:15h), so the 6h dissection point occurred at around ZT7 (between 13:55h and 14:15h), a circadian phase when Hr38 expression might be naturally elevated. In contrast, the paired learning, double-odour, and complex-odour experiments included time-of-day controls (Figs. 3C,E, 4B,D, 5B,D), ensuring that exposure occurred at different circadian phases across replicates. As a result, no time-dependent increase in Hr38 expression was observed under those conditions.

In summary, our experiments show that Hr38 abundance does not reliably reflect odour-evoked activity in Kenyon cells. Instead, fluctuations in Hr38::GFP+ Kenyon cell numbers appear to be driven by circadian influences, possibly ruling out the use of Hr38-based tools to mark Kenyon cell engrams.

However, the experiments demonstrate the robustness of our fluorescence-based pipeline for 3D quantification of variable expression among Kenyon cells. This method can be used to measure changes in protein levels in other neuronal populations, and provides a foundation for testing alternative molecular markers that may more accurately capture memory-related neuronal activity.

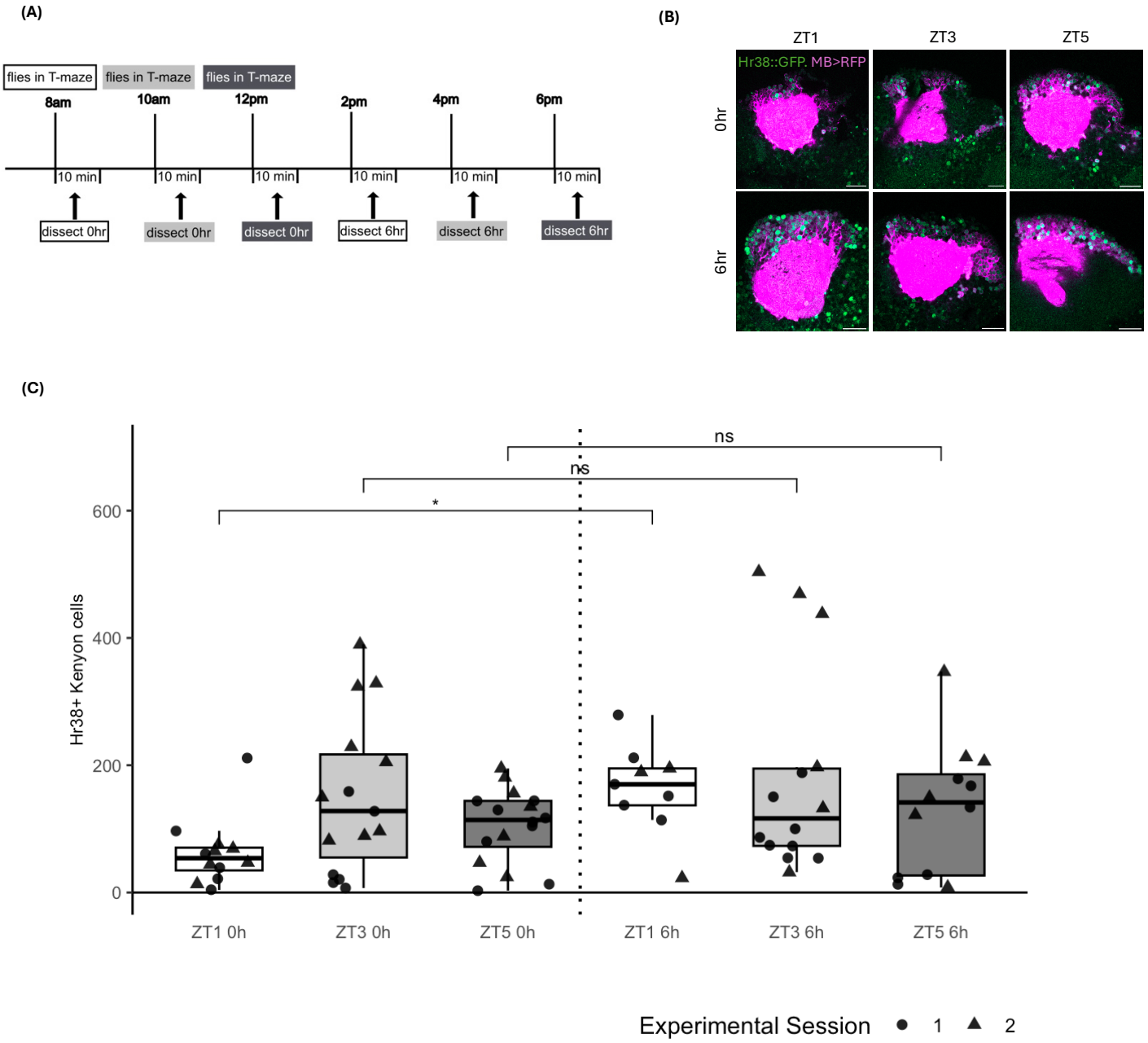

Figure 6: Hr38::GFP expression in Kenyon cells is regulated by circadian timing. (**A**) Experimental design. Flies were placed in a T-maze without odour exposure at ZT1 (08:00), ZT3 (10:00), or ZT5 (12:00h). Brains were dissected immediately or 6h later. (**B**) Representative images of brains dissected at 0h and 6h following T-maze exposure at each time point. Green, Hr38::sfGFP. Magenta, MB247-LexA, LexAop-rCD2::RFP. Scale bar, 20µm. (**C**) The number of Hr38::GFP+ Kenyon cells across time points. Flies exposed at 08:00 h showed a significant increase in Hr38+ cells at 6h compared to 0h, whereas no differences were observed at 10:00h or 12:00h. *: $p < 0.05$ (Kruskal–Wallis test). Sample sizes: 08:00h 0h, n = 11; 10:00h 0h, n = 14; 12:00h 0h, n = 15; 08:00h 6h, n = 8; 10:00h 6h, n = 13; 12:00h 6h, n = 11 (across two experimental replicates). Boxplots show minimum, Q1, median, Q3, and maximum values. Each point represents Hr38::GFP+ cell number from the right-hand calyx of one brain. Different shapes indicate independent experimental sessions.

Discussion, Conclusions and Future Directions

Principal findings

In this thesis, I described a method to automate the counting of Kenyon cells tagged with an endogenous Hr38::GFP reporter across three-dimensional image stacks using the FIJI plugin TrackMate. By optimising a GFP intensity threshold, I distinguished cells which robustly express Hr38 (Hr38::GFP+ cells) from those with only low basal levels (Hr38::GFP- cells) (Fig. 1A).

Using this approach, I asked whether GFP-tagged Hr38 could act as a reliable marker of neuronal activity in Kenyon cells. A timeline experiment revealed a striking rise in Hr38::GFP+ cells, peaking at 6h after exposure and falling back towards baseline by 10h (Fig. 2C). Whereas this dynamic apparently mirrored the transient induction expected of an ARG, the temporal dynamics were slower and the number of Hr38::GFP+ cells was higher than anticipated. My subsequent experiments revealed that the rise in Hr38::GFP+ cells only happened when flies were trained early in the day. When I trained them later, or controlled for time of day, that increase disappeared (Figs. 3E, 4D, 5D, 6C).

I did not expect the number of Hr38::GFP+ cells to differ between paired and unpaired learning. During paired learning, dopamine is released onto Kenyon cell terminals at the MBON synapse coincident with odour-evoked activity in the Kenyon cell soma (5). This coincident release drives synaptic plasticity and forms the basis of associative learning (108). In unpaired learning, dopamine release and Kenyon cell activation are not coincidental, so synaptic modification does not occur (101). There is no reason to expect that paired Kenyon cell activation and dopamine release would change the expression of an activity-regulated gene in the Kenyon cell soma differently to unpaired Kenyon cell activation and dopamine release. Nonetheless, it was important to confirm this experimentally, as establishing whether Hr38 expression varies with learning is essential before considering it as a potential engram marker.

Because complex odours, such as apple cider vinegar, are expected to activate a broader population of Kenyon cells than simple synthetic odours like MCH, a reliable activity marker should label a greater number of Kenyon cells following exposure to apple cider vinegar. Surprisingly, there was also no increase in Hr38::GFP+ Kenyon cells when flies were exposed to apple cider vinegar compared to MCH (Fig. 5D). In the experiment where flies were exposed to a mixture of two synthetic odours, the number of Hr38::GFP+ Kenyon cells increased from 0h to 6h in the double-odour group. However, this apparent increase most likely reflects inconsistent time-of-day control across experimental sessions. The double-odour group was exposed to the odour mixture early in the day in three independent sessions, whereas the single-odour groups were trained at that time only once or twice (Fig. 4B,D).

Together, these results reveal that although Hr38 is expressed in a sparse subset of Kenyon cells reminiscent of odour-evoked activation patterns, it does not report odour-evoked activity in the mushroom body. Instead, its expression is likely shaped by circadian timing. This leads to a central question: if *Hr38* is not an activity marker in Kenyon cells, what is driving its expression?

Hr38 is not a reliable activity marker in Kenyon cells

Several lines of evidence have suggested that *Hr38* expression might be controlled by neuronal activity in Kenyon cells. *Hr38* is rapidly and transiently induced in the Drosophila brain by artificial stimulation, including optogenetically, thermogenetically, and by KCl incubation (70). It has been identified as a conserved insect ARG induced by social and sensory cues, and appears in transcriptomic datasets from Kenyon cells after memory training (79,109). Moreover, *Hr38* is the Drosophila orthologue of the mammalian *Nr4A* family, which are well-established immediate early genes (the mammalian equivalent of ARGs) linked to synaptic plasticity and memory formation in rodents (110).

My results, however, show that Hr38::GFP does not reliably report odour-evoked activity in Kenyon cells. At the peak of expression in the timeline and circadian control experiments, Hr38::GFP+ cell numbers reached ~200 (Figs. 2C, 6C). This

lies at the upper end of what would be expected if odour-driven activation were being reported, as odour-responsive activity in Kenyon cells is typically limited to 5–10% of the population (about 100–200 cells per hemisphere) (5,30). Furthermore, if Hr38::GFP was reporting odour-evoked activity, I would expect protein levels to rise more rapidly. Hr38 mRNA peaks ~90 min after behavioural stimulation, and allowing for translation and nuclear localisation, peak Hr38::GFP expression would be expected to occur between 2.5 – 4h after odour exposure (79,111,112). Instead, I observed that Hr38::GFP peaked more gradually, at ~6h (Fig. 2C).

Most critically, Hr38::GFP+ cell numbers did not increase between 0h and 6h across independent experimental sessions when circadian timing was controlled (Figs. 3E, 4D, 5D). Hr38::GFP+ cell counts also did not differ between MCH, a simple, synthetic odour, and apple cider vinegar, a natural, complex odour which would be expected to activate multiple populations of Kenyon cells (104,113). Together, these findings indicate that Hr38::GFP is not reporting odour-evoked Kenyon cell activity.

There are, however, several caveats to consider. Firstly, the binary classification I used (Hr38::GFP+ vs Hr38::GFP-) may have lacked the sensitivity to capture increases in GFP levels within cells already classified as Hr38::GFP+. For instance, while qualitatively I did not observe clear differences in fluorescence between odour mixtures and single odours (Figs. 4C, 5C), it remains possible that mixtures induced subtle increases in a subset of Hr38::GFP+ cells that were masked in my counts.

Second, an important consideration when interpreting these results is the distinction between transcriptomic and protein-level measurements of gene expression. A previous study indicated that Hr38 mRNA peaks approximately 90 minutes after neuronal stimulation, consistent with its classification as an activity-regulated gene (79). In contrast, the Hr38::GFP signal measured in my experiements peaked at approximately 6 hours following odour exposure. This discrepancy does not necessarily indicate a difference in the underlying transcriptional response, but might reflect the temporal delay between transcription and detectable protein accumulation. Translation, protein folding, and nuclear localisation all contribute to this delay, and the use of a GFP tag may further extend the time required for fluorescence to become detectable due to fluorophore maturation kinetics (114–116).

Moreover, protein-based measurements integrate expression over time and are influenced by protein stability and degradation rates (115,117). As a result, Hr38::GFP fluorescence may represent a cumulative signal of prior transcriptional activity rather than a precise readout of the timing or magnitude of neuronal activation. This temporal integration could contribute to the broader and slower dynamics observed in this study, including the delayed peak and the relatively large number of Hr38::GFP+ cells.

Third, the odour stimuli I used may have been insufficient in strength or duration to cross the transcriptional threshold for Hr38 induction. ARGs typically require relatively strong or repeated stimulation, and a single 2 min exposure may not have been enough to trigger detectable Hr38 transcription, even if robust action potentials were triggered in Kenyon cells (79,118,119).

Lastly, although I carefully controlled odour presentation, other environmental cues such as pheromones, food odours, or background laboratory odours could have been detected by the flies. Such uncontrolled stimuli may have artificially elevated the number of Hr38::GFP+ cells.

Hr38 upregulation in the Kenyon cells is likely circadian-gated

My results show that the number of Hr38::GFP+ Kenyon cells varies with circadian time rather than odour-evoked activity (Fig. 6C). Although Kenyon cells are not part of the central clock circuit, there is evidence that their physiology is influenced by circadian-state signals (120,121). Because *Hr38* is an ARG requiring intracellular Ca^{2+} influx and cAMP/PKA signalling for its induction, rhythmic changes in Kenyon cell excitability could determine when *Hr38* can be upregulated (122). Mushroom body cAMP/PKA signalling and excitability are themselves under circadian control via rhythmic input from clock neurons, suggesting that windows of elevated excitability may gate *Hr38* transcription to specific circadian phases (123–125).

Some elements of cAMP/PKA pathway in the mushroom body, including *Pka-C1*, are under circadian regulation (121). Although the Zeitgeber time of maximal signalling in

Kenyon cells is not established, my sampling under a 12:12h light-dark cycle (ZT0 ≈ 07:00h) at ZT1 (≈ 08:00h), ZT7 (≈ 14:00h), and ZT11 (≈ 18:00h) covers a plausible daytime window of high mushroom body excitability (Figs. 2C, 6C). Day-peaking rhythms in cAMP, PKA and Ca^{2+} signals are clock-driven and show higher daytime than nighttime activity (124). PKA-C1 protein levels also oscillate across the day, reaching maximal abundance during the light phase in a clock-dependent manner (126). The initial number of Hr38::GFP+ cells I observed at ZT1 could coincide with the onset of a proposed daytime ramp. This ramp could peak at ZT7 to align with a mid-day high, and the decline by ZT11 to mirror a late-day fall in signalling. Circadian modulation of mushroom body physiology similarly affects sleep and learning performance, reinforcing the idea that rhythmic *Hr38* expression could reflect time-of-day-dependent variation in Kenyon cell plasticity (125,127).

How the clock circuit might act to drive transcriptional changes in the mushroom body is not known. There is no evidence that clock neurons interact directly with the mushroom body. However, there are several potential mechanisms through which the circadian system could modulate Kenyon cell excitability, thereby regulating *Hr38* transcriptional responsiveness. Firstly, if pigment dispersing factor (PDF), which is the principal circadian neuropeptide in flies, is released by the small Ventral Lateral neurons (s-LNvs) at a point which impacts any of the neurons which are extrinsic to the mushroom body, this might impact the Kenyon cell excitability downstream (128). For example, MBONs and DANs form feedback and feedforward loops with Kenyon cells, and if any of these are impacted by clock neurons, that might modify Kenyon cell excitability at different points of the day (5).

Second, crosstalk between circadian rhythms and glial activity may influence neuronal excitability in the mushroom body. In the central clock circuit, both astrocyte-like and surface glia modulate the excitability of the PDF-expressing s-LNvs that drive circadian locomotor rhythms, acting through calcium-dependent and dopamine-related mechanisms (129,130). Although direct evidence of circadian modulation of Kenyon cells is lacking, it is plausible that similar glial mechanisms could rhythmically influence mushroom body excitability.

Third, it is possible that *Hr38* integrates endocrine and circadian signals in the Kenyon cells. *Hr38* is known to participate in ecdysteroid-mediated signalling pathways and interacts with hormonal receptor complexes in *Drosophila* larvae (131,132). While direct evidence for endocrine regulation of *Hr38* in adult Kenyon cells is not yet established, adult brain hormone signalling, for example, ecdysone-dependent changes in cAMP in the mushroom body, provides a plausible route by which *Hr38* could integrate endocrine and neural signals (133). This would account for the phenomenon that *Hr38* is required for courtship LTM but seems to be dispensable in olfactory LTM (James Evans, personal communication, 130). *Hr38* was identified as one of a small set of transcription factors that are rapidly and transiently induced in the mushroom body following courtship conditioning. Functional knockdown of *Hr38* impaired long-term courtship memory, indicating that *Hr38* is required for transcriptional processes underlying memory consolidation (134). Courtship LTM in *Drosophila* is shaped by the interaction of endocrine and circadian systems. Ecdysone signalling is required for the consolidation of courtship LTM, as disruption of ecdysone receptor activity in the mushroom body impairs memory formation (135). The circadian clock gene *period* is also necessary for courtship LTM, as per^{0} mutants fail to consolidate short-term memories into long-term memories (136). Given that *Hr38* is both ecdysone-responsive in fly larvae, and my results show that it is expressed in the brain in a manner reminiscent of courtship rhythms, it is possible that *Hr38* might regulate hormonal and endocrine cues in courtship memory-related plasticity in the mushroom body.

While these hypotheses provide some avenues to explore the potential role of *Hr38* in the Kenyon cells, none of them addresses a central problem: if *Hr38* expression is linked to circadian excitability, one would expect a broad increase in Hr38::GFP fluorescence across the entire Kenyon cell population rather than the restricted subset of Hr38::GFP+ cells observed. While there is no definite answer to this question, several explanations exist.

Firstly, circadian influences on the mushroom body are unlikely to act uniformly. Clock-driven outputs are often selective, targeting specific neural populations through neuromodulators, peptidergic signalling, or defined synaptic pathways, which could confine circadian effects to particular mushroom body compartments or

Kenyon cell subtypes (125,137–139). Second, only a subset of Kenyon cells may possess the molecular components or downstream circuitry necessary to respond to circadian cues, and these responses may also depend on prior activity or chromatin state that render some cells transcriptionally “primed” (5,41,125,140,141). This functional heterogeneity would ensure that some Kenyon cells remain stable in their response to odours, independent of internal state, while others are able to respond in a circadian-responsive way, allowing time-of-day-specific learning. Functionally, this would enable the fly to perform circadian-gated forms of learning while preserving circadian-independent memory functions. Circadian modulation may therefore open a transient window of permissiveness that enables *Hr38* induction only in those Kenyon cells that are both receptive and appropriately conditioned, producing the sparse activation pattern observed rather than a global change across the mushroom body. However, these hypotheses must be tested experimentally before any conclusions can be drawn about how circadian modulation might influence *Hr38* regulation in the Kenyon cells.

Alternative candidate Kenyon cell engram markers

Previous studies have attempted to label and manipulate Kenyon cell populations involved in memory storage. One such study employed the transcription factor *CREB2* as an engram label (142). *CREB2* is an activity-responsive transcriptional activator whose function is regulated post-translationally by cAMP/PKA and Ca^{2+} signalling (9,143). Unlike an ARG, its expression is largely constitutive, and neuronal stimulation modulates its activity rather than its transcription (12,144). In this study, a tool termed “CAMEL” (CRE-Activity–Dependent Memory Engram Label) was developed using a split-Gal4 system to restrict *CRE*-driven expression to α/β surface and γ Kenyon cells, which are implicated in aversive LTM. The authors demonstrated that CAMEL selectively labelled neurons activated during spaced, but not massed, training, consistent with its dependence on *CREB2*-mediated transcription. However, the effectiveness of this system as a true engram label was limited. The labelled Kenyon cells were only transiently required for memory recall. Silencing these neurons impaired LTM expression at two and five days after training but not at seven days, indicating that the CAMEL-marked population contributes to early

consolidation or recall rather than permanent memory storage. As a true engram label should mark neurons which permanently store the memory, this is a significant limitation (145,146). Furthermore, CAMEL produced sparse and variable labelling, identifying only a few Kenyon cells per hemisphere with notable asymmetry between the right and left mushroom body hemispheres. Lastly, optogenetic activation of CAMEL-labelled neurons alone elicited only a partial avoidance response compared to natural memory recall. Together, these findings suggest that while CAMEL successfully targeted neurons transiently engaged during LTM formation, it failed to comprehensively or stably label the full engram population (142).

Another study used the immediate early gene *c-fos* (also known as *kayak* in *Drosophila*) to identify Kenyon cell populations involved in aversive LTM (147). *c-fos* encodes a transcription factor that is induced by neuronal activity through MAPK/ERK and calcium-dependent signalling cascades (140,148). Unlike *CREB2*, whose expression is largely constitutive, *c-fos* functions as a classical ARG and serves as a marker of recent neuronal activation (12,148). In this study, the authors demonstrated that *c-fos* and *CREB* form a positive feedback loop during spaced, but not massed, training, and that this mutual reinforcement is essential for establishing long-term, protein-synthesis-dependent memory. A Gal4 transcriptional reporter line driven by the *c-fos* promoter was used to label α/β Kenyon cells showing strong *c-fos* activity following training. These neurons were shown to be necessary and sufficient for memory recall 24 hours after training, consistent with their proposed role as engram neurons. However, this study did not establish that the labelled neurons showed persistence in a way that is consistent with true engrams. As they did not examine whether the same neurons remain necessary or active during recall at later time points past 24 hours, these cells might not be the permanent memory storage cells. Furthermore, *c-fos* is a broad activity-regulated gene induced by many stimuli, so *kayak-GAL4* may also label neurons active for reasons unrelated to the learned association (140,148). The labelled population was relatively large and not shown to be odour- or experience-specific. Without demonstrating that the labelled cells correspond to the small, stimulus-specific ensemble modified during learning, this approach cannot reliably identify which neurons constitute the memory trace.

As I have shown that the ARG *Hr38* is also unlikely to serve as an effective Kenyon cell engram marker, it would be advantageous to explore alternative genes which might serve as effective markers. The most likely candidate for this is the ARG *stripe* (*egr1* in mammals). *stripe* appears alongside *Hr38* in a transcriptional profiling dataset which shows both ARGs are strongly and transiently upregulated in response to neuronal stimulation (70). Like *Hr38*, *stripe* seems to be dispensable in olfactory LTM, meaning that it can likely be tagged for use as an engram marker without interfering with the memory formation itself (James Evans, personal communication). It is the *Drosophila* orthologue of the mammalian gene *erg1*, which successfully marks cells involved in the engram in mammals (149). However, the similarities it has to *Hr38* in its pattern of upregulation in response to neuronal stimulation means that it might show similar issues when being used as an engram marker (70). Performing the same experiments with stripe::GFP as I did in this project with Hr38::GFP would be a sensible next step in determining whether *stripe* could be used as an engram marker.

Other potential genes to assess include *CrebA*, *Arc1, Homer* or *Jra*. *CrebA* is induced more slowly than ARGs in response to neuronal activity, and regulates genes involved in protein synthesis and ER function, all processes which are required during later stages of LTM consolidation (70,150). As it is not an ARG and is likely required later in the memory-formation cascade, it might be used to label neurons which show changes in protein synthesis as a result of the synaptic plasticity associated with LTM formation. *Arc1* and *Homer* are synaptic plasticity-associated genes. In *Drosophila*, *Arc1* encodes a retrovirus-like capsid protein that traffics RNA between neurons and is implicated in synaptic plasticity (151). *Homer* encodes a postsynaptic scaffolding protein that organizes glutamate receptors and calcium-signalling complexes (152). Similarly to *CrebA*, tagging these genes might identify neurons undergoing structural consolidation and identify the neurons storing long-term memories. *Jra* is a component of the AP-1 transcription factor complex, along with *c-Fos*, the gene used for the CAMEL reporter (142,153,154). It has been implicated in synaptic plasticity and neuronal regulation (155). As the CAMEL reporter marks a very low number of cells, it would be worthwhile testing a different component of the AP-1 complex which might be more successful at labelling higher numbers of engram cells.

Future directions

Before pursuing mechanistic explanations for *Hr38* regulation, it will be essential to rigorously verify the validity and reproducibility of the current findings. All experiments comparing the number of Hr38::GFP+ Kenyon cells (Figs. 2, 3, 4, 5) should be repeated under stricter temporal control. Prior to recognising the influence of circadian rhythm on *Hr38* expression, flies were exposed to the experimental conditions within a ±15 min window of the intended Zeitgeber time. Although this timing variability is unlikely to account for large differences, repeating the experiments with exposures timed precisely to the appropriate ZT would remove a potential source of noise. In the double-odour experiment in particular, sampling windows must be aligned across experimental sessions. Repeating this experiment is critical for determining whether the apparent increase in Hr38::GFP+ cells between 0h and 6h in the mixed-odour group reflects a circadian bias, as we currently suspect, or whether it represents a genuine odour-dependent change (Figs. 4B, D).

In addition to these controls, methodological refinements would help to validate and extend the present findings. Increasing the number of sampling timepoints in the learning, double-odour, and complex-odour experiments (Figs. 3, 4, 5) would determine whether the 0h - 6h comparison has overlooked faster or transient changes in *Hr38* expression. More sensitive molecular approaches could also be used to verify the fluorescence-based data and reveal subtle transcriptional dynamics that fall below the detection limits of the GFP reporter. qPCR offers high sensitivity and temporal resolution for measuring changes in total *Hr38* mRNA within the mushroom body (156). Although it lacks single-cell resolution, qPCR would provide an accurate assessment of transcript level changes across timepoints and, when combined with GFP- based measurements, would give a more complete and quantitative picture of *Hr38* transcriptional dynamics than my experiments in this project have provided. Finally, blinding analyses, cross-validation of the TrackMate detection pipeline between experimenters, and statistical reporting of effect sizes with confidence intervals would enhance reproducibility and transparency. Collectively, these steps would establish whether the apparent circadian

dependence of *Hr38* reflects a true biological phenomenon or arises from methodological or sampling artefacts.

The most informative next step for determining what *Hr38* is responding to would be to compare Hr38::GFP expression in flies exposed to an odour after surgical removal of the antennae versus intact controls. Antennectomy eliminates the olfactory receptor neurons, which detect odour stimuli and relay this information to projection neurons in the antennal lobe that, in turn, synapse onto Kenyon cells (157–160). In flies lacking antennae, no olfactory receptor neuron-derived sensory input reaches the mushroom body. Thus, any Hr38 induction observed in their Kenyon cells would reflect intrinsic activity or non-olfactory influences rather than odour-evoked signalling. Another important experiment would be to remove a single antenna and compare the number of Hr38::GFP+ cells between the left and right mushroom body hemispheres. If *Hr38* responds to olfactory input, the hemisphere ipsilateral to the intact antenna should show a markedly higher number of Hr38::GFP+ Kenyon cells. Importantly, all antennal ablation experiments must include sham-wound controls to distinguish the effects of sensory deprivation from those of surgical injury or handling.

It would also be valuable to explore additional mechanistic explanations for the time-dependent regulation of *Hr38* in Kenyon cells. One approach would be to test whether the Hr38::GFP rhythm depends on output from the PDF-expressing s-LNvs. Silencing s-LNvs, either by hyperpolarising them with Kir2.1 (*pdf-Gal4* > *UAS-Kir2.1*) or by acutely blocking synaptic transmission using a temperature-sensitive *shibire* allele, would reveal whether circadian input from these neurons is required to generate the ZT-dependent fluctuations in Hr38::GFP expression (161,162). Complementarily, artificially activating the s-LNvs at timepoints when Hr38::GFP levels are typically low would test whether clock-neuron output is sufficient to open a permissive window for *Hr38* induction. This could be achieved by expressing Chrimson in PDF+ neurons (*pdf-Gal4* > *UAS-Chrimson*) and optogenetically stimulating the s-LNvs at ZT1 or ZT11, when Hr38::GFP expression normally declines (163). Finally, knocking down the PDF receptor (PDFR) using RNAi in mushroom body extrinsic neurons would test whether PDF acts indirectly on Kenyon cells via intermediary circuits. Suitable candidates for PDFR knockdown include

dopaminergic neurons, MBONs, and astrocytes. Assessing whether this manipulation flattens the Hr38::GFP rhythm would clarify whether PDF-dependent circadian signalling reaches Kenyon cells through these intermediate pathways.

To test whether hormonal signalling contributes to *Hr38* induction in Kenyon cells and whether this might explain the courtship-specific requirement for *Hr38* in LTM, it would be informative to manipulate ecdysone pathways selectively in the adult mushroom body. Adult-specific knockdown of the Ecdysone receptor (EcR) in Kenyon cells, using a *MB-Gal4, tub-GAL80^{ts} > UAS-EcR RNAi* fly line for example, would allow assessment as to whether reducing ecdysone responsiveness alters Hr38::GFP expression following olfactory or courtship conditioning. If *Hr38* upregulation is hormone-dependent, EcR knockdown should alter Hr38::GFP+ cell number dynamics after odour or courtship exposure at specific ZTs. Conversely, administering 20-hydroxyecdysone (20E) to adult flies at defined ZTs could test whether elevating systemic hormone levels is sufficient to modulate *Hr38* expression. 20E is the active steroid form of ecdysone in adult flies (164). If 20E feeding increases the number of Hr38::GFP+ Kenyon cells at ZTs in which expression is normally low (such as ZT1 or ZT11), this would indicate that *Hr38* induction is sensitive to endocrine state. Together, these experiments would clarify whether ecdysone signalling interacts with circadian phase to regulate *Hr38* dynamics in the mushroom body.

At the molecular level, profiling transcriptional and chromatin changes in *Hr38*-deficient Kenyon cells using RNA-seq or ATAC-seq would identify *Hr38*-dependent gene networks and regulatory targets. Such datasets would determine whether *Hr38* acts primarily as a transcriptional activator, a repressor, or a chromatin modulator within these neurons. Together, these unbiased functional approaches would clarify whether *Hr38* contributes to general neuronal plasticity, cell-state maintenance, or another as-yet-uncharacterised process in the mushroom body.

Finally, an important avenue for future work will be to use transcriptional markers that more reliably label neurons participating in long-term memory engrams to actually demonstrate that these engram cells are activated during both memory formation and memory recall. To this end, we have designed a genetic construct which could be used on candidate engram-marker genes once their upregulation

patterns in the Kenyon cells following odour-induced activation have been profiled. The *candidate gene:T2A:Gal4; hsFLP* × *UAS>GFP>RFP; tub-GAL80^{ts}* construct will enable temporally restricted labelling of neurons expressing the gene during both training and memory recall. In this system, the candidate gene-driven Gal4 activity during training induces GFP expression in Kenyon cells, marking those active during memory formation. Subsequent heat shock before testing will trigger Flp-mediated recombination, such that any new gene expression during memory recall drives RFP expression. Overlap between GFP- and RFP-labelled populations would identify neurons reactivated during recall, indicating re-engagement of the same transcriptional program that was active during encoding (Fig. 7A). While our data suggest *Hr38* is unlikely to fulfil this role, this approach could be applied to other candidate activity-regulated genes, such as *stripe*, *CrebA, homer, Arc1* or *Jra* to identify transcriptional markers that more faithfully report experience-dependent neuronal activation.

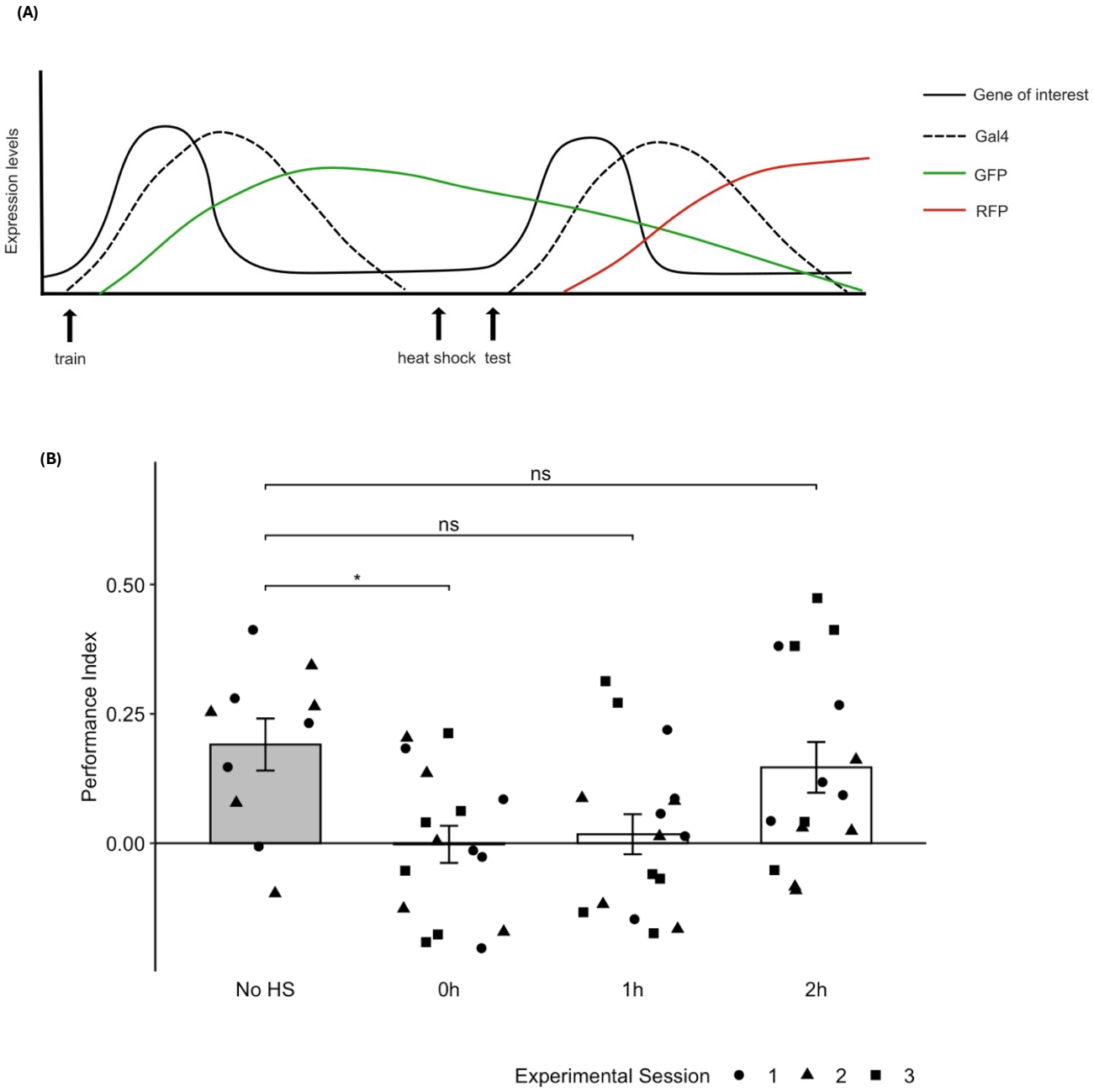

Figure 7: Design of a dual-labelling system to identify engram candidate neurons. (**A**) *candidate gene:T2A:Gal4; hsFLP × UAS>GFP>RFP; tub-GAL80^{ts}* kenyon cell dual-labelling fly line design. During training, the gene of interest is upregulated in the cells in response to the odour. Simultaneously, Gal4 is translated and cleaved, which drives the production of GFP. ~21 hours later, flies are heat-shocked, which triggers a recombination event and causes Gal4 to drive RFP production instead. Then, during testing, where Kenyon cells are again activated by the odour, the cells will express RFP. Cells which have been activated by both events should express both GFP and RFP. (**B**) LTM appetitive memory scores comparing CS flies which have not received a heat shock to those which have been heat shocked for an hour at 37°C either directly before training or one or two hours prior to training. *: $p < 0.05$ (Kruskal–Wallis test). Sample sizes: No HS, n = 10; 0h, n = 16; 1h, n = 16; 2h, n = 15 (across three experimental sessions). Error bars represent SEM. Different shapes indicate independent experimental sessions.

have shown that memory performance is not significantly different between heat-shocked and non-heat-shocked flies within one hour, although the data seems to trend towards better recovery by two hours. (Fig. 7B). This establishes two hours post-heat-shock as a suitable recovery window for applying the dual-labelling paradigm without disrupting behavioural performance. Future work could therefore adapt this system to test candidate genes under identical training and testing conditions to determine which exhibit stable, reactivated expression patterns consistent with engram labelling.

Complementary approaches could refine this search further. Transcriptional reporters for *stripe*, *CrebA*, *homer, Arc1*, or *Jra* could be combined with functional calcium imaging to verify that reporter induction corresponds to neuronal reactivation. Integrating these reporters with tools for neural silencing or activation such as *UAS-shibire^{ts}* or *UAS-TrpA1* would test whether reactivation of reporter-labelled neurons is necessary or sufficient for behavioural recall, thereby providing causal evidence for engram identity. Together, these experiments would define a molecular signature of memory-associated Kenyon cells and identify a new generation of candidate engram markers for the Drosophila mushroom body.

Conclusions

Together, the findings presented in this project refine our understanding of *Hr38* function in the *Drosophila* mushroom body. Although *Hr38* has previously been considered an ARG, the results here demonstrate that its expression in Kenyon cells is not driven by odour-evoked neuronal activation. Instead, Hr38 levels vary systematically with time of day, revealing that its induction is likely to be shaped primarily by circadian phase rather than sensory input. This challenges the assumption that *Hr38* is upregulated in response to neuronal activity in the mushroom body and instead positions it as an indicator of internal physiological state. By demonstrating that Hr38::GFP is unsuitable as an activity or engram marker in Kenyon cells, this study underscores the need to identify alternative molecular reporters that faithfully track neuronal recruitment during learning and memory retrieval.

Crucially, this work was made possible by the imaging-analysis pipeline developed in this project, which combines region-of-interest masking with automated spot detection to quantify Hr38::GFP expression across the entire Kenyon cell population. This approach enabled unbiased, high-throughput comparison of transcriptional responses across conditions and revealed patterns that would not have been evident from qualitative inspection alone. These methodological advances, together with the design of a temporally controlled dual-labelling reporter system, provide new tools for interrogating transcriptional dynamics in identified neuronal populations.

Ultimately, this work contributes to a growing recognition that memory formation in *Drosophila* is shaped not only by synaptic activity but also by the organism's intrinsic physiological milieu, including its circadian phase, hormonal environment, and prior experience. Understanding how these internal signals intersect with circuit-level plasticity will be essential for explaining how memories are encoded, stabilised, and retrieved across different contexts. The experimental tools and analytical framework developed here lay the groundwork for future investigations into discovering transcriptional markers that more accurately represent memory-encoding neurons in the mushroom body.

Bibliography

1. Josselyn SA, Köhler S, Frankland PW. Finding the engram. Nat Rev Neurosci. 2015 Sep;16(9):521–34. doi:10.1038/nrn4000 PubMed PMID: 26289572.

2. Semon R. The Mneme London [Internet]. 1921 [cited 2024 Nov 25]. Available from: https://scholar.google.com/scholar_lookup?&title=The%20Mneme&publication_year=1921&author=Semon%2CR#d=gs_cit&t=1732553490645&u=%2Fscholar%3Fq%3Dinfo%3Ah_tIaBB5rdwJ%3Ascholar.google.com%2F%26output%3Dcite%26scirp%3D0%26hl%3Den

3. Pang B, Wu X, Chen H, Yan Y, Du Z, Yu Z, et al. Exploring the memory: existing activity-dependent tools to tag and manipulate engram cells. Front Cell Neurosci. 2023;17:1279032. doi:10.3389/fncel.2023.1279032 PubMed PMID: 38259503; PubMed Central PMCID: PMC10800721.

4. Tully T, Quinn WG. Classical conditioning and retention in normal and mutant Drosophila melanogaster. J Comp Physiol [A]. 1985 Sep;157(2):263–77. doi:10.1007/BF01350033 PubMed PMID: 3939242.

5. Aso Y, Hattori D, Yu Y, Johnston RM, Iyer NA, Ngo TTB, et al. The neuronal architecture of the mushroom body provides a logic for associative learning. eLife. 2014 Dec 23;3:e04577. doi:10.7554/eLife.04577 PubMed PMID: 25535793; PubMed Central PMCID: PMC4273437.

6. Pavlov (1927) PI. Conditioned reflexes: An investigation of the physiological activity of the cerebral cortex. Ann Neurosci. 2010 Jul;17(3):136–41. doi:10.5214/ans.0972-7531.1017309 PubMed PMID: 25205891; PubMed Central PMCID: PMC4116985.

7. Pandey UB, Nichols CD. Human disease models in Drosophila melanogaster and the role of the fly in therapeutic drug discovery. Pharmacol Rev. 2011 Jun;63(2):411–36. doi:10.1124/pr.110.003293 PubMed PMID: 21415126; PubMed Central PMCID: PMC3082451.

8. Levin LR, Han PL, Hwang PM, Feinstein PG, Davis RL, Reed RR. The Drosophila learning and memory gene rutabaga encodes a Ca2+/Calmodulin-responsive adenylyl cyclase. Cell. 1992 Feb 7;68(3):479–89. doi:10.1016/0092-8674(92)90185-f PubMed PMID: 1739965.

9. Lonze BE, Ginty DD. Function and Regulation of CREB Family Transcription Factors in the Nervous System. Neuron. 2002 Aug 15;35(4):605–23. doi:10.1016/S0896-6273(02)00828-0 PubMed PMID: 12194863.

10. Schultz W, Dayan P, Montague PR. A neural substrate of prediction and reward. Science. 1997 Mar 14;275(5306):1593–9. doi:10.1126/science.275.5306.1593 PubMed PMID: 9054347.

11. Aso Y, Sitaraman D, Ichinose T, Kaun KR, Vogt K, Belliart-Guérin G, et al. Mushroom body output neurons encode valence and guide memory-based action selection in Drosophila. eLife. 2014 Dec 23;3:e04580. doi:10.7554/eLife.04580 PubMed PMID: 25535794; PubMed Central PMCID: PMC4273436.

12. Yin JC, Wallach JS, Del Vecchio M, Wilder EL, Zhou H, Quinn WG, et al. Induction of a dominant negative CREB transgene specifically blocks long-term memory in Drosophila. Cell. 1994 Oct 7;79(1):49–58. doi:10.1016/0092-8674(94)90399-9 PubMed PMID: 7923376.

13. Silva AJ, Kogan JH, Frankland PW, Kida S. CREB and memory. Annu Rev Neurosci. 1998;21:127–48. doi:10.1146/annurev.neuro.21.1.127 PubMed PMID: 9530494.

14. Schlegel P, Yin Y, Bates AS, Dorkenwald S, Eichler K, Brooks P, et al. Whole-brain annotation and multi-connectome cell typing of Drosophila. Nature. 2024 Oct;634(8032):139–52. doi:10.1038/s41586-024-07686-5

15. Zheng Z, Lauritzen JS, Perlman E, Robinson CG, Nichols M, Milkie D, et al. A Complete Electron Microscopy Volume of the Brain of Adult Drosophila melanogaster. Cell. 2018 Jul 26;174(3):730-743.e22. doi:10.1016/j.cell.2018.06.019 PubMed PMID: 30033368.

16. Brand AH, Perrimon N. Targeted gene expression as a means of altering cell fates and generating dominant phenotypes. Development. 1993 Jun 1;118(2):401–15. doi:10.1242/dev.118.2.401

17. Dietzl G, Chen D, Schnorrer F, Su KC, Barinova Y, Fellner M, et al. A genome-wide transgenic RNAi library for conditional gene inactivation in Drosophila. Nature. 2007 Jul;448(7150):151–6. doi:10.1038/nature05954

18. Claridge-Chang A, Roorda RD, Vrontou E, Sjulson L, Li H, Hirsh J, et al. Writing Memories with Light-Addressable Reinforcement Circuitry. Cell. 2009 Oct 16;139(2):405–15. doi:10.1016/j.cell.2009.08.034 PubMed PMID: 19837039.

19. Akerboom J, Chen TW, Wardill TJ, Tian L, Marvin JS, Mutlu S, et al. Optimization of a GCaMP Calcium Indicator for Neural Activity Imaging. J Neurosci. 2012 Oct 3;32(40):13819–40. doi:10.1523/JNEUROSCI.2601-12.2012 PubMed PMID: 23035093.

20. Davis RL. OLFACTORY MEMORY FORMATION IN DROSOPHILA: From Molecular to Systems Neuroscience. Annu Rev Neurosci. 2005 Jul 21;28(Volume 28, 2005):275–302. doi:10.1146/annurev.neuro.28.061604.135651

21. Krashes MJ, Waddell S. Rapid consolidation to a radish and protein synthesis-dependent long-term memory after single-session appetitive olfactory conditioning in Drosophila. J Neurosci Off J Soc Neurosci. 2008 Mar 19;28(12):3103–13. doi:10.1523/JNEUROSCI.5333-07.2008 PubMed PMID: 18354013; PubMed Central PMCID: PMC2516741.

22. Tully T, Preat T, Boynton SC, Del Vecchio M. Genetic dissection of consolidated memory in Drosophila. Cell. 1994 Oct 7;79(1):35–47. doi:10.1016/0092-8674(94)90398-0 PubMed PMID: 7923375.

23. Pascual A, Préat T. Localization of long-term memory within the Drosophila mushroom body. Science. 2001 Nov 2;294(5544):1115–7. doi:10.1126/science.1064200 PubMed PMID: 11691997.

24. Tanaka NK, Tanimoto H, Ito K. Neuronal assemblies of the Drosophila mushroom body. J Comp Neurol. 2008 Jun 10;508(5):711–55. doi:10.1002/cne.21692 PubMed PMID: 18395827.

25. Heisenberg M. Mushroom body memoir: from maps to models. Nat Rev Neurosci. 2003 Apr;4(4):266–75. doi:10.1038/nrn1074

26. Clyne PJ, Warr CG, Freeman MR, Lessing D, Kim J, Carlson JR. A novel family of divergent seven-transmembrane proteins: candidate odorant receptors in Drosophila. Neuron. 1999 Feb;22(2):327–38. doi:10.1016/s0896-6273(00)81093-4 PubMed PMID: 10069338.

27. Wang Y, Guo HF, Pologruto TA, Hannan F, Hakker I, Svoboda K, et al. Stereotyped odor-evoked activity in the mushroom body of Drosophila revealed by green fluorescent protein-based Ca2+ imaging. J Neurosci Off J Soc Neurosci. 2004 Jul 21;24(29):6507–14. doi:10.1523/JNEUROSCI.3727-03.2004 PubMed PMID: 15269261; PubMed Central PMCID: PMC6729867.

28. Couto A, Alenius M, Dickson BJ. Molecular, anatomical, and functional organization of the Drosophila olfactory system. Curr Biol CB. 2005 Sep 6;15(17):1535–47. doi:10.1016/j.cub.2005.07.034 PubMed PMID: 16139208.

29. Fishilevich E, Vosshall LB. Genetic and functional subdivision of the Drosophila antennal lobe. Curr Biol CB. 2005 Sep 6;15(17):1548–53. doi:10.1016/j.cub.2005.07.066 PubMed PMID: 16139209.

30. Turner GC, Bazhenov M, Laurent G. Olfactory representations by Drosophila mushroom body neurons. J Neurophysiol. 2008 Feb;99(2):734–46. doi:10.1152/jn.01283.2007 PubMed PMID: 18094099.

31. Honegger KS, Campbell RAA, Turner GC. Cellular-resolution population imaging reveals robust sparse coding in the Drosophila mushroom body. J Neurosci Off J Soc Neurosci. 2011 Aug 17;31(33):11772–85. doi:10.1523/JNEUROSCI.1099-11.2011 PubMed PMID: 21849538; PubMed Central PMCID: PMC3180869.

32. Owald D, Felsenberg J, Talbot CB, Das G, Perisse E, Huetteroth W, et al. Activity of defined mushroom body output neurons underlies learned olfactory behavior in Drosophila. Neuron. 2015 Apr 22;86(2):417–27. doi:10.1016/j.neuron.2015.03.025 PubMed PMID: 25864636; PubMed Central PMCID: PMC4416108.

33. Perisse E, Owald D, Barnstedt O, Talbot CB, Huetteroth W, Waddell S. Aversive Learning and Appetitive Motivation Toggle Feed-Forward Inhibition in the Drosophila Mushroom Body. Neuron. 2016 Jun 1;90(5):1086–99.

doi:10.1016/j.neuron.2016.04.034 PubMed PMID: 27210550; PubMed Central PMCID: PMC4893166.

34. Burke CJ, Huetteroth W, Owald D, Perisse E, Krashes MJ, Das G, et al. Layered reward signalling through octopamine and dopamine in Drosophila. Nature. 2012 Dec 20;492(7429):433–7. doi:10.1038/nature11614 PubMed PMID: 23103875; PubMed Central PMCID: PMC3528794.

35. Hige T, Aso Y, Modi MN, Rubin GM, Turner GC. Heterosynaptic Plasticity Underlies Aversive Olfactory Learning in Drosophila. Neuron. 2015 Dec 2;88(5):985–98. doi:10.1016/j.neuron.2015.11.003 PubMed PMID: 26637800; PubMed Central PMCID: PMC4674068.

36. Liu C, Plaçais PY, Yamagata N, Pfeiffer BD, Aso Y, Friedrich AB, et al. A subset of dopamine neurons signals reward for odour memory in Drosophila. Nature. 2012 Aug 23;488(7412):512–6. doi:10.1038/nature11304 PubMed PMID: 22810589.

37. Waddell S. Reinforcement signalling in Drosophila; dopamine does it all after all. Curr Opin Neurobiol. 2013 Jun;23(3):324–9. doi:10.1016/j.conb.2013.01.005 PubMed PMID: 23391527; PubMed Central PMCID: PMC3887340.

38. Yamagata N, Ichinose T, Aso Y, Plaçais PY, Friedrich AB, Sima RJ, et al. Distinct dopamine neurons mediate reward signals for short- and long-term memories. Proc Natl Acad Sci U S A. 2015 Jan 13;112(2):578–83. doi:10.1073/pnas.1421930112 PubMed PMID: 25548178; PubMed Central PMCID: PMC4299218.

39. Owald D, Waddell S. Olfactory learning skews mushroom body output pathways to steer behavioral choice in Drosophila. Curr Opin Neurobiol. 2015 Dec;35:178–84. doi:10.1016/j.conb.2015.10.002 PubMed PMID: 26496148; PubMed Central PMCID: PMC4835525.

40. Tanaka NK, Tanimoto H, Ito K. Neuronal assemblies of the Drosophila mushroom body. J Comp Neurol. 2008 Jun 10;508(5):711–55. doi:10.1002/cne.21692 PubMed PMID: 18395827.

41. Li F, Lindsey JW, Marin EC, Otto N, Dreher M, Dempsey G, et al. The connectome of the adult Drosophila mushroom body provides insights into function. eLife. 2020 Dec 14;9:e62576. doi:10.7554/eLife.62576 PubMed PMID: 33315010; PubMed Central PMCID: PMC7909955.

42. Zars T, Wolf R, Davis R, Heisenberg M. Tissue-Specific Expression of a Type I Adenylyl Cyclase Rescues the rutabaga Mutant Memory Defect: In Search of the Engram. Learn Mem. 2000 Jan;7(1):18–31. PubMed PMID: 10706599; PubMed Central PMCID: PMC311318.

43. Yu D, Akalal DBG, Davis RL. Drosophila alpha/beta mushroom body neurons form a branch-specific, long-term cellular memory trace after spaced olfactory conditioning. Neuron. 2006 Dec 7;52(5):845–55.

doi:10.1016/j.neuron.2006.10.030 PubMed PMID: 17145505; PubMed Central PMCID: PMC1779901.

44. Krashes MJ, Keene AC, Leung B, Armstrong JD, Waddell S. Sequential use of mushroom body neuron subsets during drosophila odor memory processing. Neuron. 2007 Jan 4;53(1):103–15. doi:10.1016/j.neuron.2006.11.021 PubMed PMID: 17196534; PubMed Central PMCID: PMC1828290.

45. Blum AL, Li W, Cressy M, Dubnau J. Short and Long-term memory in Drosophila require cAMP signaling in distinct neuron types. Curr Biol CB. 2009 Aug 25;19(16):1341–50. doi:10.1016/j.cub.2009.07.016 PubMed PMID: 19646879; PubMed Central PMCID: PMC2752374.

46. Trannoy S, Redt-Clouet C, Dura JM, Preat T. Parallel processing of appetitive short- and long-term memories in Drosophila. Curr Biol CB. 2011 Oct 11;21(19):1647–53. doi:10.1016/j.cub.2011.08.032 PubMed PMID: 21962716.

47. Qin H, Cressy M, Li W, Coravos JS, Izzi SA, Dubnau J. Gamma neurons mediate dopaminergic input during aversive olfactory memory formation in Drosophila. Curr Biol CB. 2012 Apr 10;22(7):608–14. doi:10.1016/j.cub.2012.02.014 PubMed PMID: 22425153; PubMed Central PMCID: PMC3326180.

48. Huetteroth W, Perisse E, Lin S, Klappenbach M, Burke C, Waddell S. Sweet taste and nutrient value subdivide rewarding dopaminergic neurons in Drosophila. Curr Biol CB. 2015 Mar 16;25(6):751–8. doi:10.1016/j.cub.2015.01.036 PubMed PMID: 25728694; PubMed Central PMCID: PMC4372253.

49. Ichinose T, Aso Y, Yamagata N, Abe A, Rubin GM, Tanimoto H. Reward signal in a recurrent circuit drives appetitive long-term memory formation. eLife. 2015 Nov 17;4:e10719. doi:10.7554/eLife.10719 PubMed PMID: 26573957; PubMed Central PMCID: PMC4643015.

50. Bailey CH, Kandel ER. Structural changes accompanying memory storage. Annu Rev Physiol. 1993;55:397–426. doi:10.1146/annurev.ph.55.030193.002145 PubMed PMID: 8466181.

51. Kandel ER. The molecular biology of memory storage: a dialogue between genes and synapses. Science. 2001 Nov 2;294(5544):1030–8. doi:10.1126/science.1067020 PubMed PMID: 11691980.

52. Malinow R, Malenka RC. AMPA receptor trafficking and synaptic plasticity. Annu Rev Neurosci. 2002;25:103–26. doi:10.1146/annurev.neuro.25.112701.142758 PubMed PMID: 12052905.

53. Yang G, Pan F, Gan WB. Stably maintained dendritic spines are associated with lifelong memories. Nature. 2009 Dec;462(7275):920–4. doi:10.1038/nature08577

54. Hige T, Aso Y, Modi MN, Rubin GM, Turner GC. Heterosynaptic Plasticity Underlies Aversive Olfactory Learning in Drosophila. Neuron. 2015 Dec

2;88(5):985–98. doi:10.1016/j.neuron.2015.11.003 PubMed PMID: 26637800; PubMed Central PMCID: PMC4674068.

55. Hong EJ, McCord AE, Greenberg ME. A biological function for the neuronal activity-dependent component of Bdnf transcription in the development of cortical inhibition. Neuron. 2008 Nov 26;60(4):610–24. doi:10.1016/j.neuron.2008.09.024 PubMed PMID: 19038219; PubMed Central PMCID: PMC2873221.

56. Lin Y, Bloodgood BL, Hauser JL, Lapan AD, Koon AC, Kim TK, et al. Activity-dependent regulation of inhibitory synapse development by Npas4. Nature. 2008 Oct 30;455(7217):1198–204. doi:10.1038/nature07319 PubMed PMID: 18815592; PubMed Central PMCID: PMC2637532.

57. Bloodgood BL, Sharma N, Browne HA, Trepman AZ, Greenberg ME. The activity-dependent transcription factor NPAS4 regulates domain-specific inhibition. Nature. 2013 Nov 7;503(7474):121–5. doi:10.1038/nature12743 PubMed PMID: 24201284; PubMed Central PMCID: PMC4169177.

58. West AE, Greenberg ME. Neuronal activity-regulated gene transcription in synapse development and cognitive function. Cold Spring Harb Perspect Biol. 2011 Jun 1;3(6):a005744. doi:10.1101/cshperspect.a005744 PubMed PMID: 21555405; PubMed Central PMCID: PMC3098681.

59. Spiegel I, Mardinly A, Gabel H, Bazinet J, Couch C, Tzeng C, et al. Npas4 regulates excitatory-inhibitory balance within neural circuits through cell type-specific gene programs. Cell. 2014 May 22;157(5):1216–29. doi:10.1016/j.cell.2014.03.058 PubMed PMID: 24855953; PubMed Central PMCID: PMC4089405.

60. Fowler T, Sen R, Roy AL. Regulation of primary response genes. Mol Cell. 2011 Nov 4;44(3):348–60. doi:10.1016/j.molcel.2011.09.014 PubMed PMID: 22055182; PubMed Central PMCID: PMC3212756.

61. Kida S, Josselyn SA, Peña de Ortiz S, Kogan JH, Chevere I, Masushige S, et al. CREB required for the stability of new and reactivated fear memories. Nat Neurosci. 2002 Apr;5(4):348–55. doi:10.1038/nn819 PubMed PMID: 11889468.

62. Bourtchuladze R, Frenguelli B, Blendy J, Cioffi D, Schutz G, Silva AJ. Deficient long-term memory in mice with a targeted mutation of the cAMP-responsive element-binding protein. Cell. 1994 Oct 7;79(1):59–68. doi:10.1016/0092-8674(94)90400-6 PubMed PMID: 7923378.

63. Pittenger C, Huang YY, Paletzki RF, Bourtchouladze R, Scanlin H, Vronskaya S, et al. Reversible inhibition of CREB/ATF transcription factors in region CA1 of the dorsal hippocampus disrupts hippocampus-dependent spatial memory. Neuron. 2002 Apr 25;34(3):447–62. doi:10.1016/s0896-6273(02)00684-0 PubMed PMID: 11988175.

64. Miyashita T, Kikuchi E, Horiuchi J, Saitoe M. Long-Term Memory Engram Cells Are Established by c-Fos/CREB Transcriptional Cycling. Cell Rep. 2018 Dec

4;25(10):2716-2728.e3. doi:10.1016/j.celrep.2018.11.022 PubMed PMID: 30517860.

65. Tomchik SM, Davis RL. Dynamics of learning-related cAMP signaling and stimulus integration in the Drosophila olfactory pathway. Neuron. 2009 Nov 25;64(4):510–21. doi:10.1016/j.neuron.2009.09.029 PubMed PMID: 19945393; PubMed Central PMCID: PMC4080329.

66. Gervasi N, Tchénio P, Preat T. PKA dynamics in a Drosophila learning center: coincidence detection by rutabaga adenylyl cyclase and spatial regulation by dunce phosphodiesterase. Neuron. 2010 Feb 25;65(4):516–29. doi:10.1016/j.neuron.2010.01.014 PubMed PMID: 20188656.

67. Livingstone MS, Sziber PP, Quinn WG. Loss of calcium/calmodulin responsiveness in adenylate cyclase of rutabaga, a Drosophila learning mutant. Cell. 1984 May;37(1):205–15. doi:10.1016/0092-8674(84)90316-7 PubMed PMID: 6327051.

68. Impey S, Obrietan K, Storm DR. Making new connections: role of ERK/MAP kinase signaling in neuronal plasticity. Neuron. 1999 May;23(1):11–4. doi:10.1016/s0896-6273(00)80747-3 PubMed PMID: 10402188.

69. Alberini C, Taubenfeld SM, Garcia-Osta A. CREB and the CREB-C/EBP-dependent gene expression cascade in long-term memory. Cellscience Rev. 2005;2.

70. Chen X, Rahman R, Guo F, Rosbash M. Genome-wide identification of neuronal activity-regulated genes in Drosophila. Bellen HJ, editor. eLife. 2016 Dec 9;5:e19942. doi:10.7554/eLife.19942

71. Fowler T, Sen R, Roy AL. Regulation of primary response genes. Mol Cell. 2011 Nov 4;44(3):348–60. doi:10.1016/j.molcel.2011.09.014 PubMed PMID: 22055182; PubMed Central PMCID: PMC3212756.

72. Rosen JB, Fanselow MS, Young SL, Sitcoske M, Maren S. Immediate-early gene expression in the amygdala following footshock stress and contextual fear conditioning. Brain Res. 1998 Jun 15;796(1–2):132–42. doi:10.1016/s0006-8993(98)00294-7 PubMed PMID: 9689463.

73. Guzowski JF, McNaughton BL, Barnes CA, Worley PF. Environment-specific expression of the immediate-early gene Arc in hippocampal neuronal ensembles. Nat Neurosci. 1999 Dec;2(12):1120–4. doi:10.1038/16046 PubMed PMID: 10570490.

74. Minatohara K, Akiyoshi M, Okuno H. Role of Immediate-Early Genes in Synaptic Plasticity and Neuronal Ensembles Underlying the Memory Trace. Front Mol Neurosci. 2015;8:78. doi:10.3389/fnmol.2015.00078 PubMed PMID: 26778955; PubMed Central PMCID: PMC4700275.

75. Miyashita T, Kikuchi E, Horiuchi J, Saitoe M. Long-Term Memory Engram Cells Are Established by c-Fos/CREB Transcriptional Cycling. Cell Rep. 2018 Dec

4;25(10):2716-2728.e3. doi:10.1016/j.celrep.2018.11.022 PubMed PMID: 30517860.

76. King-Jones K, Thummel CS. Nuclear receptors — a perspective from Drosophila. Nat Rev Genet. 2005 Apr;6(4):311–23. doi:10.1038/nrg1581

77. Kozlova T, Pokholkova GV, Tzertzinis G, Sutherland JD, Zhimulev IF, Kafatos FC. Drosophila Hormone Receptor 38 Functions in Metamorphosis: A Role in Adult Cuticle Formation. Genetics. 1998 Jul 1;149(3):1465–75. doi:10.1093/genetics/149.3.1465

78. Kozlova T, Thummel CS. Essential roles for ecdysone signaling during Drosophila mid-embryonic development. Science. 2003 Sep 26;301(5641):1911–4. doi:10.1126/science.1087419 PubMed PMID: 12958367.

79. Fujita N, Nagata Y, Nishiuchi T, Sato M, Iwami M, Kiya T. Visualization of Neural Activity in Insect Brains Using a Conserved Immediate Early Gene, Hr38. Curr Biol. 2013 Oct 21;23(20):2063–70. doi:10.1016/j.cub.2013.08.051 PubMed PMID: 24120640.

80. Singh AS, Shah A, Brockmann A. Honey bee foraging induces upregulation of early growth response protein 1, hormone receptor 38 and candidate downstream genes of the ecdysteroid signalling pathway. Insect Mol Biol. 2018 Feb;27(1):90–8. doi:10.1111/imb.12350 PubMed PMID: 28987007.

81. Iino S, Shiota Y, Nishimura M, Asada S, Ono M, Kubo T. Neural activity mapping of bumble bee (Bombus ignitus) brains during foraging flight using immediate early genes. Sci Rep. 2020 May 12;10(1):7887. doi:10.1038/s41598-020-64701-1 PubMed PMID: 32398802; PubMed Central PMCID: PMC7217898.

82. Ugajin A, Uchiyama H, Miyata T, Sasaki T, Yajima S, Ono M. Identification and initial characterization of novel neural immediate early genes possibly differentially contributing to foraging-related learning and memory processes in the honeybee. Insect Mol Biol. 2018 Apr;27(2):154–65. doi:10.1111/imb.12355 PubMed PMID: 29096051.

83. Hawk JD, Abel T. The role of NR4A transcription factors in memory formation. Brain Res Bull. 2011 Apr 25;85(1–2):21–9. doi:10.1016/j.brainresbull.2011.02.001 PubMed PMID: 21316423; PubMed Central PMCID: PMC3078984.

84. Bridi MS, Hawk JD, Chatterjee S, Safe S, Abel T. Pharmacological Activators of the NR4A Nuclear Receptors Enhance LTP in a CREB/CBP-Dependent Manner. Neuropsychopharmacol Off Publ Am Coll Neuropsychopharmacol. 2017 May;42(6):1243–53. doi:10.1038/npp.2016.253 PubMed PMID: 27834392; PubMed Central PMCID: PMC5437882.

85. Flavell SW, Cowan CW, Kim TK, Greer PL, Lin Y, Paradis S, et al. Activity-dependent regulation of MEF2 transcription factors suppresses excitatory synapse number. Science. 2006 Feb 17;311(5763):1008–12. doi:10.1126/science.1122511 PubMed PMID: 16484497.

86. Shalizi A, Gaudillière B, Yuan Z, Stegmüller J, Shirogane T, Ge Q, et al. A calcium-regulated MEF2 sumoylation switch controls postsynaptic differentiation. Science. 2006 Feb 17;311(5763):1012–7. doi:10.1126/science.1122513 PubMed PMID: 16484498.

87. Adhikari P, Orozco D, Randhawa H, Wolf FW. Mef2 induction of the immediate early gene Hr38/Nr4a is terminated by Sirt1 to promote ethanol tolerance. Genes Brain Behav. 2019 Mar;18(3):e12486. doi:10.1111/gbb.12486 PubMed PMID: 29726098; PubMed Central PMCID: PMC6215524.

88. Krashes MJ, Waddell S. Rapid consolidation to a radish and protein synthesis-dependent long-term memory after single-session appetitive olfactory conditioning in Drosophila. J Neurosci Off J Soc Neurosci. 2008 Mar 19;28(12):3103–13. doi:10.1523/JNEUROSCI.5333-07.2008 PubMed PMID: 18354013; PubMed Central PMCID: PMC2516741.

89. Campbell RAA, Honegger KS, Qin H, Li W, Demir E, Turner GC. Imaging a population code for odor identity in the Drosophila mushroom body. J Neurosci Off J Soc Neurosci. 2013 Jun 19;33(25):10568–81. doi:10.1523/JNEUROSCI.0682-12.2013 PubMed PMID: 23785169; PubMed Central PMCID: PMC3685844.

90. Aso Y, Hattori D, Yu Y, Johnston RM, Iyer NA, Ngo TT, et al. The neuronal architecture of the mushroom body provides a logic for associative learning. Griffith LC, editor. eLife. 2014 Dec 23;3:e04577. doi:10.7554/eLife.04577

91. Pitman JL, Huetteroth W, Burke CJ, Krashes MJ, Lai SL, Lee T, et al. A pair of inhibitory neurons are required to sustain labile memory in the Drosophila mushroom body. Curr Biol CB. 2011 May 24;21(10):855–61. doi:10.1016/j.cub.2011.03.069 PubMed PMID: 21530258; PubMed Central PMCID: PMC3111962.

92. Jiang SA, Campusano JM, Su H, O'Dowd DK. Drosophila Mushroom Body Kenyon Cells Generate Spontaneous Calcium Transients Mediated by PLTX-Sensitive Calcium Channels. J Neurophysiol. 2005 Jul;94(1):491–500. doi:10.1152/jn.00096.2005

93. Harrell ER, Pimentel D, Miesenböck G. Changes in Presynaptic Gene Expression during Homeostatic Compensation at a Central Synapse. J Neurosci Off J Soc Neurosci. 2021 Apr 7;41(14):3054–67. doi:10.1523/JNEUROSCI.2979-20.2021 PubMed PMID: 33608385; PubMed Central PMCID: PMC8026347.

94. Apostolopoulou AA, Lin AC. Mechanisms underlying homeostatic plasticity in the Drosophila mushroom body in vivo. Proc Natl Acad Sci. 2020 Jul 14;117(28):16606–15. doi:10.1073/pnas.1921294117

95. Lin HW, Chen CC, de Belle JS, Tully T, Chiang AS. CREBA and CREBB in two identified neurons gate long-term memory formation in Drosophila. Proc Natl Acad Sci. 2021 Sep 14;118(37):e2100624118. doi:10.1073/pnas.2100624118

96. Takayanagi-Kiya S, Kiya T. Activity-dependent visualization and control of neural circuits for courtship behavior in the fly Drosophila melanogaster. Proc Natl Acad Sci. 2019 Mar 19;116(12):5715–20. doi:10.1073/pnas.1814628116

97. Watanabe K, Chiu H, Anderson DJ. Whole-brain in situ mapping of neuronal activation in Drosophila during social behaviors and optogenetic stimulation. Beckwith EJ, Cardona A, editors. eLife. 2024 Nov 28;12:RP92380. doi:10.7554/eLife.92380

98. Tinevez JY, Perry N, Schindelin J, Hoopes GM, Reynolds GD, Laplantine E, et al. TrackMate: An open and extensible platform for single-particle tracking. Methods. 2017 Feb 15;Image Processing for Biologists115:80–90. doi:10.1016/j.ymeth.2016.09.016

99. Adhikari P, Orozco D, Randhawa H, Wolf FW. Mef2 induction of the immediate early gene Hr38/Nr4a is terminated by Sirt1 to promote ethanol tolerance. Genes Brain Behav. 2019 Mar;18(3):e12486. doi:10.1111/gbb.12486 PubMed PMID: 29726098; PubMed Central PMCID: PMC6215524.

100. Handler A, Graham TGW, Cohn R, Morantte I, Siliciano AF, Zeng J, et al. Distinct Dopamine Receptor Pathways Underlie the Temporal Sensitivity of Associative Learning. Cell. 2019 Jun 27;178(1):60-75.e19. doi:10.1016/j.cell.2019.05.040 PubMed PMID: 31230716; PubMed Central PMCID: PMC9012144.

101. Boto T, Louis T, Jindachomthong K, Jalink K, Tomchik SM. Dopaminergic Modulation of cAMP Drives Nonlinear Plasticity across the *Drosophila* Mushroom Body Lobes. Curr Biol. 2014 Apr 14;24(8):822–31. doi:10.1016/j.cub.2014.03.021

102. Dylla KV, Hong EJ. Mapping Odor to Action: (Dopaminergic) Timing Is Everything. Cell. 2019 Jun 27;178(1):5–7. doi:10.1016/j.cell.2019.06.010

103. Gruntman E, Turner GC. Integration of the olfactory code across dendritic claws of single mushroom body neurons. Nat Neurosci. 2013 Dec;16(12):1821–9. doi:10.1038/nn.3547

104. Guiné RPF, Barroca MJ, Coldea TE, Bartkiene E, Anjos O. Apple Fermented Products: An Overview of Technology, Properties and Health Effects. Processes. 2021 Feb;9(2):223. doi:10.3390/pr9020223

105. Lüdke A, Raiser G, Nehrkorn J, Herz AVM, Galizia CG, Szyszka P. Calcium in Kenyon Cell Somata as a Substrate for an Olfactory Sensory Memory in Drosophila. Front Cell Neurosci. 2018 May 14;12. doi:10.3389/fncel.2018.00128

106. Faucher CP, Hilker M, Bruyne M de. Interactions of Carbon Dioxide and Food Odours in Drosophila: Olfactory Hedonics and Sensory Neuron Properties. PLOS ONE. 2013 Feb 15;8(2):e56361. doi:10.1371/journal.pone.0056361

107. Endo K, Tsuchimoto Y, Kazama H. Synthesis of Conserved Odor Object Representations in a Random, Divergent-Convergent Network. Neuron. 2020 Oct 28;108(2):367-381.e5. doi:10.1016/j.neuron.2020.07.029

108. Handler A, Graham TGW, Cohn R, Morantte I, Siliciano AF, Zeng J, et al. Distinct Dopamine Receptor Pathways Underlie the Temporal Sensitivity of Associative Learning. Cell. 2019 Jun 27;178(1):60-75.e19. doi:10.1016/j.cell.2019.05.040 PubMed PMID: 31230716.

109. Jones SG, Nixon KCJ, Chubak MC, Kramer JM. Mushroom Body Specific Transcriptome Analysis Reveals Dynamic Regulation of Learning and Memory Genes After Acquisition of Long-Term Courtship Memory in Drosophila. G3 Bethesda Md. 2018 Nov 6;8(11):3433–46. doi:10.1534/g3.118.200560 PubMed PMID: 30158319; PubMed Central PMCID: PMC6222587.

110. Hawk JD, Abel T. The role of NR4A transcription factors in memory formation. Brain Res Bull. 2011 Apr 25;Novel principles underlying memory formation85(1):21–9. doi:10.1016/j.brainresbull.2011.02.001

111. Harris JA. Using c-*fos* as a Neural Marker of Pain. Brain Res Bull. 1998 Jan 1;45(1):1–8. doi:10.1016/S0361-9230(97)00277-3

112. Bojovic O, Panja D, Bittins M, Bramham CR, Tjølsen A. Time Course of Immediate Early Gene Protein Expression in the Spinal Cord following Conditioning Stimulation of the Sciatic Nerve in Rats. PLOS ONE. 2015 Apr 10;10(4):e0123604. doi:10.1371/journal.pone.0123604

113. Perisse E, Yin Y, Lin AC, Lin S, Huetteroth W, Waddell S. Different kenyon cell populations drive learned approach and avoidance in Drosophila. Neuron. 2013 Sep 4;79(5):945–56. doi:10.1016/j.neuron.2013.07.045 PubMed PMID: 24012007; PubMed Central PMCID: PMC3765960.

114. Heim R, Prasher DC, Tsien RY. Wavelength mutations and posttranslational autoxidation of green fluorescent protein. Proc Natl Acad Sci. 1994 Dec 20;91(26):12501–4. doi:10.1073/pnas.91.26.12501

115. Vogel C, Marcotte EM. Insights into the regulation of protein abundance from proteomic and transcriptomic analyses. Nat Rev Genet. 2012 Apr;13(4):227–32. doi:10.1038/nrg3185

116. Balleza E, Kim JM, Cluzel P. Systematic characterization of maturation time of fluorescent proteins in living cells. Nat Methods. 2018 Jan;15(1):47–51. doi:10.1038/nmeth.4509 PubMed PMID: 29320486; PubMed Central PMCID: PMC5765880.

117. Liu Y, Beyer A, Aebersold R. On the Dependency of Cellular Protein Levels on mRNA Abundance. Cell. 2016 Apr 21;165(3):535–50. doi:10.1016/j.cell.2016.03.014 PubMed PMID: 27104977.

118. Morgan JI, Curran T. Stimulus-transcription coupling in neurons: role of cellular immediate-early genes. Trends Neurosci. 1989 Nov;12(11):459–62. doi:10.1016/0166-2236(89)90096-9 PubMed PMID: 2479148.

119. Herrera DG, Robertson HA. Activation of c-fos in the brain. Prog Neurobiol. 1996 Oct;50(2–3):83–107. doi:10.1016/s0301-0082(96)00021-4 PubMed PMID: 8971979.

120. Driscoll M, Buchert SN, Coleman V, McLaughlin M, Nguyen A, Sitaraman D. Compartment specific regulation of sleep by mushroom body requires GABA and dopaminergic signaling. Sci Rep. 2021 Oct 8;11(1):20067. doi:10.1038/s41598-021-99531-2

121. Solis BL, Nagoshi E. Circadian control of dopaminergic signaling to the mushroom body regulates sleep through rhythmic Pka-C1 transcription in Drosophila [Internet]. bioRxiv; 2025 [cited 2025 Nov 8]. p. 2025.08.29.673050. Available from: https://www.biorxiv.org/content/10.1101/2025.08.29.673050v1 doi:10.1101/2025.08.29.673050

122. Aso Y, Ray RP, Long X, Bushey D, Cichewicz K, Ngo TT, et al. Nitric oxide acts as a cotransmitter in a subset of dopaminergic neurons to diversify memory dynamics. VijayRaghavan K, Ramaswami M, Strauss RH, editors. eLife. 2019 Nov 14;8:e49257. doi:10.7554/eLife.49257

123. Fujii S, Krishnan P, Hardin P, Amrein H. Nocturnal male sex drive in Drosophila. Curr Biol CB. 2007 Feb 6;17(3):244–51. doi:10.1016/j.cub.2006.11.049 PubMed PMID: 17276917; PubMed Central PMCID: PMC2239012.

124. Guo F, Cerullo I, Chen X, Rosbash M. PDF neuron firing phase-shifts key circadian activity neurons in Drosophila. Ptáček L, editor. eLife. 2014 Jun 17;3:e02780. doi:10.7554/eLife.02780

125. King AN, Barber AF, Smith AE, Dreyer AP, Sitaraman D, Nitabach MN, et al. A Peptidergic Circuit Links the Circadian Clock to Locomotor Activity. Curr Biol CB. 2017 Jul 10;27(13):1915-1927.e5. doi:10.1016/j.cub.2017.05.089 PubMed PMID: 28669757; PubMed Central PMCID: PMC5698909.

126. Machado Almeida P, Lago Solis B, Stickley L, Feidler A, Nagoshi E. Neurofibromin 1 in mushroom body neurons mediates circadian wake drive through activating cAMP–PKA signaling. Nat Commun. 2021 Oct 1;12(1):5758. doi:10.1038/s41467-021-26031-2

127. Krzeptowski W, Hess G, Pyza E. Circadian Plasticity in the Brain of Insects and Rodents. Front Neural Circuits. 2018 May 2;12. doi:10.3389/fncir.2018.00032

128. Renn SCP, Park JH, Rosbash M, Hall JC, Taghert PH. A pdf Neuropeptide Gene Mutation and Ablation of PDF Neurons Each Cause Severe Abnormalities of Behavioral Circadian Rhythms in Drosophila. Cell. 1999 Dec 23;99(7):791–802. doi:10.1016/S0092-8674(00)81676-1 PubMed PMID: 10619432.

129. Suh J, Jackson FR. Drosophila ebony activity is required in glia for the circadian regulation of locomotor activity. Neuron. 2007 Aug 2;55(3):435–47. doi:10.1016/j.neuron.2007.06.038 PubMed PMID: 17678856; PubMed Central PMCID: PMC2034310.

130. Ng FS, Tangredi MM, Jackson FR. Glial cells physiologically modulate clock neurons and circadian behavior in a calcium-dependent manner. Curr Biol CB. 2011 Apr 26;21(8):625–34. doi:10.1016/j.cub.2011.03.027 PubMed PMID: 21497088; PubMed Central PMCID: PMC3081987.

131. Baker KD, Shewchuk LM, Kozlova T, Makishima M, Hassell A, Wisely B, et al. The Drosophila Orphan Nuclear Receptor DHR38 Mediates an Atypical Ecdysteroid Signaling Pathway. Cell. 2003 Jun 13;113(6):731–42. doi:10.1016/S0092-8674(03)00420-3 PubMed PMID: 12809604.

132. Kozlova T, Pokholkova GV, Tzertzinis G, Sutherland JD, Zhimulev IF, Kafatos FC. Drosophila Hormone Receptor 38 Functions in Metamorphosis: A Role in Adult Cuticle Formation. Genetics. 1998 Jul 1;149(3):1465–75. doi:10.1093/genetics/149.3.1465

133. Ishimoto H, Wang Z, Rao Y, Wu CF, Kitamoto T. A Novel Role for Ecdysone in Drosophila Conditioned Behavior: Linking GPCR-Mediated Non-canonical Steroid Action to cAMP Signaling in the Adult Brain. PLOS Genet. 2013 Oct 10;9(10):e1003843. doi:10.1371/journal.pgen.1003843

134. Jones SG, Gil-Martí B, Sacristán-Horcajada E, Edison AC, Butler EF, Miandashti N, et al. A memory transcriptome time course reveals essential long-term memory transcription factors. Nat Commun. 2025 Oct 29;16(1):9320. doi:10.1038/s41467-025-64379-x

135. Ishimoto H, Sakai T, Kitamoto T. Ecdysone signaling regulates the formation of long-term courtship memory in adult Drosophila melanogaster. Proc Natl Acad Sci U S A. 2009 Apr 14;106(15):6381–6. doi:10.1073/pnas.0810213106 PubMed PMID: 19342482; PubMed Central PMCID: PMC2669368.

136. Sakai T, Tamura T, Kitamoto T, Kidokoro Y. A clock gene, period, plays a key role in long-term memory formation in Drosophila. Proc Natl Acad Sci U S A. 2004 Nov 9;101(45):16058–63. doi:10.1073/pnas.0401472101 PubMed PMID: 15522971; PubMed Central PMCID: PMC528738.

137. Shafer OT, Yao Z. Pigment-Dispersing Factor Signaling and Circadian Rhythms in Insect Locomotor Activity. Curr Opin Insect Sci. 2014 Jul 1;1:73–80. doi:10.1016/j.cois.2014.05.002 PubMed PMID: 25386391; PubMed Central PMCID: PMC4224320.

138. Helfrich-Förster C. Organization of endogenous clocks in insects. Biochem Soc Trans. 2005 Nov;33(Pt 5):957–61. doi:10.1042/BST20050957 PubMed PMID: 16246020.

139. Liang X, Holy TE, Taghert PH. Synchronous Drosophila circadian pacemakers display nonsynchronous Ca^{2+} rhythms in vivo. Science. 2016 Feb 26;351(6276):976–81. doi:10.1126/science.aad3997 PubMed PMID: 26917772; PubMed Central PMCID: PMC4836443.

140. West AE, Greenberg ME. Neuronal Activity–Regulated Gene Transcription in Synapse Development and Cognitive Function. Cold Spring Harb Perspect Biol. 2011 Jan 6;3(6):a005744. doi:10.1101/cshperspect.a005744

141. Tyssowski KM, Gray JM. The neuronal stimulation-transcription coupling map. Curr Opin Neurobiol. 2019 Dec;59:87–94. doi:10.1016/j.conb.2019.05.001 PubMed PMID: 31163285; PubMed Central PMCID: PMC6885097.

142. Siegenthaler D, Escribano B, Bräuler V, Pielage J. Selective suppression and recall of long-term memories in Drosophila. PLoS Biol. 2019 Aug;17(8):e3000400. doi:10.1371/journal.pbio.3000400 PubMed PMID: 31454345; PubMed Central PMCID: PMC6711512.

143. Montminy M. TRANSCRIPTIONAL REGULATION BY CYCLIC AMP. Annu Rev Biochem. 1997 Jul 1;66(Volume 66, 1997):807–22. doi:10.1146/annurev.biochem.66.1.807

144. Silva AJ, Kogan JH, Frankland PW, Kida S. CREB AND MEMORY. Annu Rev Neurosci. 1998 Mar 1;21(Volume 21, 1998):127–48. doi:10.1146/annurev.neuro.21.1.127

145. Tonegawa S, Liu X, Ramirez S, Redondo R. Memory Engram Cells Have Come of Age. Neuron. 2015 Sep 2;87(5):918–31. doi:10.1016/j.neuron.2015.08.002

146. Josselyn SA, Köhler S, Frankland PW. Finding the engram. Nat Rev Neurosci. 2015 Sep;16(9):521–34. doi:10.1038/nrn4000

147. Miyashita T, Kikuchi E, Horiuchi J, Saitoe M. Long-Term Memory Engram Cells Are Established by c-Fos/CREB Transcriptional Cycling. Cell Rep. 2018 Dec 4;25(10):2716-2728.e3. doi:10.1016/j.celrep.2018.11.022 PubMed PMID: 30517860.

148. Sheng M, Greenberg ME. The regulation and function of c-fos and other immediate early genes in the nervous system. Neuron. 1990 Apr 1;4(4):477–85. doi:10.1016/0896-6273(90)90106-P PubMed PMID: 1969743.

149. Reijmers LG, Perkins BL, Matsuo N, Mayford M. Localization of a Stable Neural Correlate of Associative Memory. Science. 2007 Aug 31;317(5842):1230–3. doi:10.1126/science.1143839

150. Fox RM, Hanlon CD, Andrew DJ. The CrebA/Creb3-like transcription factors are major and direct regulators of secretory capacity. J Cell Biol. 2010 Nov 1;191(3):479–92. doi:10.1083/jcb.201004062 PubMed PMID: 21041443; PubMed Central PMCID: PMC3003312.

151. Ashley J, Cordy B, Lucia D, Fradkin LG, Budnik V, Thomson T. Retrovirus-like Gag Protein Arc1 Binds RNA and Traffics across Synaptic Boutons. Cell. 2018 Jan 11;172(1–2):262-274.e11. doi:10.1016/j.cell.2017.12.022 PubMed PMID: 29328915; PubMed Central PMCID: PMC5793882.

152. Diagana TT, Thomas U, Prokopenko SN, Xiao B, Worley PF, Thomas JB. Mutation of Drosophila homer Disrupts Control of Locomotor Activity and Behavioral Plasticity. J Neurosci. 2002 Jan 15;22(2):428–36. doi:10.1523/JNEUROSCI.22-02-00428.2002 PubMed PMID: 11784787; PubMed Central PMCID: PMC6758666.

153. Kockel L, Homsy JG, Bohmann D. Drosophila AP-1: lessons from an invertebrate. Oncogene. 2001 Apr;20(19):2347–64. doi:10.1038/sj.onc.1204300

154. Perkins KK, Admon A, Patel N, Tjian R. The Drosophila Fos-related AP-1 protein is a developmentally regulated transcription factor. Genes Dev. 1990 May;4(5):822–34. doi:10.1101/gad.4.5.822 PubMed PMID: 2116361.

155. Sanyal S, Sandstrom DJ, Hoeffer CA, Ramaswami M. AP-1 functions upstream of CREB to control synaptic plasticity in Drosophila. Nature. 2002 Apr 25;416(6883):870–4. doi:10.1038/416870a PubMed PMID: 11976688.

156. Bustin SA. Absolute quantification of mRNA using real-time reverse transcription polymerase chain reaction assays. J Mol Endocrinol. 2000 Oct;25(2):169–93. doi:10.1677/jme.0.0250169 PubMed PMID: 11013345.

157. de Bruyne M, Foster K, Carlson JR. Odor coding in the Drosophila antenna. Neuron. 2001 May;30(2):537–52. doi:10.1016/s0896-6273(01)00289-6 PubMed PMID: 11395013.

158. Stocker RF. The organization of the chemosensory system in Drosophila melanogaster: a review. Cell Tissue Res. 1994 Jan;275(1):3–26. doi:10.1007/BF00305372 PubMed PMID: 8118845.

159. Marin EC, Jefferis GSXE, Komiyama T, Zhu H, Luo L. Representation of the glomerular olfactory map in the Drosophila brain. Cell. 2002 Apr 19;109(2):243–55. doi:10.1016/s0092-8674(02)00700-6 PubMed PMID: 12007410.

160. Turner GC, Bazhenov M, Laurent G. Olfactory representations by Drosophila mushroom body neurons. J Neurophysiol. 2008 Feb;99(2):734–46. doi:10.1152/jn.01283.2007 PubMed PMID: 18094099.

161. Grigliatti TA, Hall L, Rosenbluth R, Suzuki DT. Temperature-sensitive mutations in Drosophila melanogaster. XIV. A selection of immobile adults. Mol Gen Genet MGG. 1973 Jan 24;120(2):107–14. doi:10.1007/BF00267238 PubMed PMID: 4631264.

162. Wu Y, Cao G, Nitabach MN. Electrical silencing of PDF neurons advances the phase of non-PDF clock neurons in Drosophila. J Biol Rhythms. 2008 Apr;23(2):117–28. doi:10.1177/0748730407312984 PubMed PMID: 18375861.

163. Klapoetke NC, Murata Y, Kim SS, Pulver SR, Birdsey-Benson A, Cho YK, et al. Independent optical excitation of distinct neural populations. Nat Methods. 2014 Mar;11(3):338–46. doi:10.1038/nmeth.2836 PubMed PMID: 24509633; PubMed Central PMCID: PMC3943671.

164. Riddiford L. Hormones and Drosophila development. 1993 Jan 1.